Compared with the previous methods, VWF73 has several advantages. First, it is the only ADAMTS-13–specific substrate obtained by bacterial expression system. For an enzymatic assay to measure ADAMTS-13 activity, protease-free VWF should be purified from human plasma. To overcome this obstacle, the bacterial recombinant expression system is one of the most convenient alternative methods. Whole VWF, however, is not suitable because of its large size and many disulfide bonds. Therefore, short and soluble VWF73 will be a good molecule for this purpose. Second, VWF73 can be used with N- and C-terminal tag sequences, which are often used for convenient purification and detection. Here, we used both an N-terminal GST-tag and C-terminal H-tag for purification and the GST-tag for immunodetection. These tags could be used to develop a new assay system suitable for clinical usage. Third, no denaturing reagents such as urea or guanidine-HCl as used in the previous methods are needed to cleave VWF73 efficiently. To use whole VWF as a substrate, pretreatment with high concentrations of urea or guanidine-HCl and/or carrying out the proteolytic reaction in the presence of the denaturing reagents is required. VWF73 is efficiently cleaved by ADAMTS-13 in the absence of these reagents, therefore undesired damage on the enzyme can be avoided.

As far as we examined, no significant discrepancy in the plasma ADAMTS-13 activity could be found between assays using intact VWF multimers (multimer analysis) and recombinant VWF73. The discrepancies, however, could be found in the future, because the ADAMTS-13 mutants with different activity against intact VWF and VWF73 may be identified. Alternatively, the autoantibody inhibitors in acquired TTP patients might bind the protease and interfere with recognition of large VWF but not VWF73.

In general, a specific chromogenic assay for each protease is useful for routine clinical measurement. Therefore, trials to find a chromogenic oligopeptide substrate for ADAMTS-13 were carried out but were not successful,[41] suggesting that the cleavage at Y1605-M1606 of VWF depends on not only specific residues in the close vicinity of the scissile bond but also some more remote sequences in the VWF subunit. The present study was quite consistent with this assumption. VWF73 (D1596-R1668, substrate IV in Figure 1) was a good substrate for ADAMTS-13, whereas D1596-R1659 (substrate V) was not degraded, indicating that 9 residues between E1660 and R1668 contain essential residues for cleavage. This region may contribute to the structural preservation of the cleavage site for ADAMTS-13 or interact directly with the protease. This will be interesting from the viewpoint of the enzymology of metalloproteases. In order to further define the role of residues E1660 to R1668, we tested whether substrate V could be cleaved by normal plasma in the presence of 1 to 100 μM nonapeptide, EAPDLVLQRR (corresponding to E1660-R1668 of VWF), but substrate V was not still cleaved (data not shown). The nonapeptide also had no effect on the cleavage of VWF73, suggesting that the region may not bind directly to ADAMTS-13 but contribute to proper presentation of the cleavage site to ADAMTS-13.

Causative mutations of the *ADAMTS13* gene have been identified in patients with congenital TTP.[14-18] In addition, we identified a common missense single-nucleotide polymorphism, P475S, with approximately 5% allele frequency in the Japanese population.[15] When this mutant was transiently expressed in cultured cells, it was efficiently secreted from cells like the wild-type molecule but exhibited low VWF-cleaving activity. This suggested that approximately 10% of the Japanese population (heterozygotes of P475S) may possess significantly reduced activity of ADAMTS-13 with the normal antigen level. Other unknown common genetic variations or environmental factors might be involved in abnormal activity of ADAMTS-13. In these cases, enzymatic assays to measure the ADAMTS-13 activity will be more important than the measurement of the antigen levels. Although the almost complete loss of the ADAMTS-13 activity results in TTP, the weakened ADAMTS-13 activity may also be a risk factor for some thrombotic complications due to circulating large VWF multimers. In fact, a recent report suggested decreased levels of the ADAMTS-13 activity in coronary heart disease.[42] Well-designed and large-scale studies to assess the relation between ADAMTS-13 and disease will be one of the most important issues in this field.

In conclusion, we here identified the minimal specific substrate for ADAMTS-13, VWF73, which could be a powerful tool to establish clinical enzymatic assays. We strongly hope that it will be widely used and contribute to improving the prognosis and prevention of TTP.

Acknowledgment

We thank Ms Yuko Nobe for her technical assistance.

References

1. Moschcowitz E. Hyaline thombosis of the terminal arterioles and capillaries; a hitherto undescribed disease. Proc N Y Pathol Soc. 1924;24:21-24.
2. Kinoshita S, Yoshioka A, Park YD, et al. Upshaw-Schulman syndrome revisited: a concept of congenital thrombotic thrombocytopenic purpura. Int J Hematol. 2001;74:101-108.
3. Fujimura Y, Titani K. Structure and function of von Willebrand factor. In: Bloom AL, Forbes CD, Thomas DP, Tuddenham EGD, eds. Haemostasis and Thrombosis. New York, NY: Churchill Livingstone; 1994:379-395.
4. Furlan M. Von Willebrand factor: molecular size and functional activity. Ann Hematol. 1996;72: 341-348.
5. Ruggeri ZM. von Willebrand factor. *J Clin Invest.* 1997;99:559-564.
6. Sadler JE. Biochemistry and genetics of von Willebrand factor. Annu Rev Biochem. 1998;67:395-424.
7. Chung DW, Fujikawa K. Processing of von Willebrand factor by ADAMTS-13. Biochemistry. 2002;41:11065-11070.
8. Fujimura Y, Matsumoto M, Yagi H, Yoshioka A, Matsui T, Titani K. Von Willebrand factor-cleaving protease and Upshaw-Schulman syndrome. Int J Hematol. 2002;75:25-34.
9. George JN, Sadler JE, Lämmle B. Platelets: thrombotic thrombocytopenic purpura. Hematology (Am Soc Hematol Educ Program). 2002:315-334.
10. Zheng X, Majerus EM, Sadler JE. ADAMTS13 and TTP. Curr Opin Hematol. 2002;9:389-394.
11. Tsai HM. Platelet activation and the formation of the platelet plug: deficiency of ADAMTS13 causes thrombotic thrombocytopenic purpura. Arterioscler Thromb Vasc Biol. 2003;23:388-396.
12. Kalafatis M, Takahashi Y, Girma JP, Meyer D. Localization of a collagen-interactive domain of human von Willebrand factor between amino acid residues Gly 911 and Glu 1,365. Blood. 1987;70: 1577-1583.
13. Federici AB, Bader R, Pagani S, Colibretti ML, De Marco L, Mannucci PM. Binding of von Willebrand factor to glycoproteins Ib and IIb/IIIa complex: affinity is related to multimeric size. Br J Haematol. 1989;73:93-99.
14. Levy GG, Nichols WC, Lian EC, et al. Mutations in a member of the ADAMTS gene family cause thrombotic thrombocytopenic purpura. Nature. 2001;413:488-494.
15. Kokame K, Matsumoto M, Soejima K, et al. Mutations and common polymorphisms in ADAMTS13 gene responsible for von Willebrand factor-cleaving protease activity. Proc Natl Acad Sci U S A. 2002;99:11902-11907.
16. Schneppenheim R, Budde U, Oyen F, et al. von Willebrand factor cleaving protease and ADAMTS13 mutations in childhood TTP. Blood. 2003;101:1845-1850.
17. Savasan S, Lee SK, Ginsburg D, Tsai HM. ADAMTS13 gene mutation in congenital thrombotic thrombocytopenic purpura with previously reported normal VWF cleaving protease activity. Blood. 2003;101:4449-4451.
18. Antoine G, Zimmermann K, Plaimauer B, et al. ADAMTS13 gene defects in two brothers with

constitutional thrombotic thrombocytopenic purpura and normalization of von Willebrand factor-cleaving protease activity by recombinant human ADAMTS13. Br J Haematol. 2003;120:821-824.

19. Furlan M, Robles R, Galbusera M, et al. von Willebrand factor-cleaving protease in thrombotic thrombocytopenic purpura and the hemolytic-uremic syndrome. N Engl J Med. 1998;339:1578-1584.
20. Tsai HM, Lian EC. Antibodies to von Willebrand factor-cleaving protease in acute thrombotic thrombocytopenic purpura. N Engl J Med. 1998; 339:1585-1594.
21. Fujikawa K, Suzuki H, McMullen B, Chung D. Purification of human von Willebrand factor-cleaving protease and its identification as a new member of the metalloproteinase family. Blood. 2001;98: 1662-1666.
22. Gerritsen HE, Robles R, Lämmle B, Furlan M. Partial amino acid sequence of purified von Willebrand factor-cleaving protease. Blood. 2001;98: 1654-1661.
23. Soejima K, Mimura N, Hirashima M, et al. A novel human metalloprotease synthesized in the liver and secreted into the blood: possibly, the von Willebrand factor-cleaving protease? J Biochem. 2001;130:475-480.
24. Zheng X, Chung D, Takayama TK, Majerus EM, Sadler JE, Fujikawa K. Structure of von Willebrand factor-cleaving protease (ADAMTS13), a metalloprotease involved in thrombotic thrombocytopenic purpura. J Biol Chem. 2001;276: 41059-41063.
25. Plaimauer B, Zimmermann K, Volkel D, et al. Cloning, expression, and functional characterization of the von Willebrand factor-cleaving protease (ADAMTS13). Blood. 2002;100:3626-3632.
26. Cal S, Obaya AJ, Llamazares M, Garabaya C, Quesada V, López-Otín C. Cloning, expression analysis, and structural characterization of seven novel human ADAMTSs, a family of metalloproteinases with disintegrin and thrombospondin-1 domains. Gene. 2002;283:49-62.
27. Zheng X, Nishio K, Majerus EM, Sadler JE. Cleavage of von Willebrand factor requires the spacer domain of the metalloprotease ADAMTS13. J Biol Chem. 2003;278:30136-30141.
28. Soejima K, Matsumoto M, Kokame K, et al. ADAMTS-13 cysteine-rich/spacer domains are functionally essential for von Willebrand factor cleavage. Blood. 2003;102:3232-3237.
29. Dent JA, Berkowitz SD, Ware J, Kasper CK, Ruggeri ZM. Identification of a cleavage site directing the immunochemical detection of molecular abnormalities in type IIA von Willebrand factor. Proc Natl Acad Sci U S A. 1990;87:6306-6310.
30. Tsai HM, Sussman II, Nagel RL. Shear stress enhances the proteolysis of von Willebrand factor in normal plasma. Blood. 1994;83:2171-2179.
31. Furlan M, Robles R, Lämmle B. Partial purification and characterization of a protease from human plasma cleaving von Willebrand factor to fragments produced by in vivo proteolysis. Blood. 1996;87:4223-4234.
32. Tsai HM. Physiologic cleavage of von Willebrand factor by a plasma protease is dependent on its conformation and requires calcium ion. Blood. 1996;87:4235-4244.
33. Bianchi V, Robles R, Alberio L, Furlan M, Lämmle B. Von Willebrand factor-cleaving protease (ADAMTS13) in thrombocytopenic disorders: a severely deficient activity is specific for thrombotic thrombocytopenic purpura. Blood. 2002;100:710-713.
34. Tsai HM. Is severe deficiency of ADAMTS-13 specific for thrombotic thrombocytopenic purpura? Yes. J Thromb Haemost. 2003;1:625-631.
35. Sugio Y, Okamura T, Shimoda K, et al. Ticlopidine-associated thrombotic thrombocytopenic purpura with an IgG-type inhibitor to von Willebrand factor-cleaving protease activity. Int J Hematol. 2001;74:347-351.
36. Orimo S, Ozawa E, Yagi H, Ishizashi H, Matsumoto M, Fujimura Y. Simple plasma exchange reduced autoantibody to von Willebrand factor-cleaving protease in a Japanese man with ticlopidine-associated thrombotic thrombocytopenic purpura. J Intern Med. 2002;251:280-281.
37. Mori Y, Wada H, Gabazza EC, et al. Predicting response to plasma exchange in patients with thrombotic thrombocytopenic purpura with measurement of vWF-cleaving protease activity. Transfusion. 2002;42:572-580.
38. Gerritsen HE, Turecek PL, Schwarz HP, Lämmle B, Furlan M. Assay of von Willebrand factor (vWF)-cleaving protease based on decreased collagen binding affinity of degraded vWF: a tool for the diagnosis of thrombotic thrombocytopenic purpura (TTP). Thromb Haemost. 1999;82:1386-1389.
39. Obert B, Tout H, Veyradier A, Fressinaud E, Meyer D, Girma JP. Estimation of the von Willebrand factor-cleaving protease in plasma using monoclonal antibodies to vWF. Thromb Haemost. 1999;82:1382-1385.
40. Böhm M, Vigh T, Scharrer I. Evaluation and clinical application of a new method for measuring activity of von Willebrand factor-cleaving metalloprotease (ADAMTS13). Ann Hematol. 2002;81: 430-435.
41. Furlan M, Lämmle B. Assays of von Willebrand factor-cleaving protease: a test for diagnosis of familial and acquired thrombotic thrombocytopenic purpura. Semin Thromb Hemost. 2002;28: 167-172.
42. Yoo G, Blomback M, Schenck-Gustafsson K, He S. Decreased levels of von Willebrand factor-cleaving protease in coronary heart disease and thrombotic thrombocytopenic purpura: study of a simplified method for assaying the enzyme activity based on ristocetin-induced platelet aggregation. Br J Haematol. 2003;121:123-129.

Genetic Defects Leading to Hereditary Thrombotic Thrombocytopenic Purpura

Koichi Kokame and Toshiyuki Miyata

In patients with thrombotic thrombocytopenic purpura (TTP), unusually large multimers of von Willebrand factor (VWF) circulate in the plasma. This is caused by a functional deficiency of VWF-cleaving protease, ADAMTS-13. Although TTP usually occurs as an acquired form due to autoantibodies against ADAMTS-13, the condition may be inherited in an *autosomal recessive* fashion. Thus far, genomic DNA from 23 patients with hereditary TTP and their families has been analyzed and 33 causative mutations identified in the *ADAMTS13* gene: 19 missense, five nonsense, five frameshift, and four splice mutations. Common missense polymorphisms have been also found, one of which significantly reduces ADAMTS-13 activity. No cases have been found without mutations in the *ADAMTS13* gene, suggesting that genetic defects in *ADAMTS13* are the dominant cause of hereditary TTP. Further analysis may reveal the genetic background associated with acquired TTP and other thrombotic diseases.
Semin Hematol 41:34-40.

THROMBOTIC thrombocytopenic purpura (TTP) is a highly lethal disease characterized by five features: thrombocytopenia, microangiopathic hemolytic anemia, renal failure, fever, and neurological dysfunction.[1] In TTP, platelet thrombi form within the microvasculature, which is thought to be caused by accumulation of unusually large multimers of von Willebrand factor (VWF). The majority of TTP is acquired, often affecting adolescents and adults. In a smaller number of cases, TTP is inherited in an autosomal recessive fashion, and hereditary TTP with neonatal onset and frequent relapses is often diagnosed as Upshaw-Schulman syndrome.[2]

VWF is synthesized primarily in vascular endothelial cells and secreted into the plasma as large multimeric forms.[3-6] Normally, the large multimers are cleaved into smaller forms by a plasma metalloprotease, ADAMTS-13,[7-11] which is a member of the ADAMTS (a disintegrin-like and metalloprotease [reprolysin type] with thrombospondin type 1 motif) gene family. In acquired TTP, autoantibodies against ADAMTS-13 are produced that inhibit the VWF-cleaving activity of ADAMTS-13, leading to the accumulation of highly active large VWF multimers.[12,13] In contrast, patients with hereditary TTP innately have no plasma ADAMTS-13 activity. Thus far, 33 causative mutations have been identified in the *ADAMTS13* gene and here we summarize the genetic defects leading to hereditary TTP. We describe the gene symbol of ADAMTS-13 as *ADAMTS13*, according to gene nomenclature provided by the Human Gene Nomenclature Committee. We refer to the protein as ADAMTS-13 according to recommendation of Dr Suneel S. Apte (http://www.lerner.ccf.org/bme/apte/adamts/nomenclature.php).

Structural Properties of ADAMTS-13

Human ADAMTS-13 was purified from plasma[14-16] and its cDNA was cloned.[16-18] At the same time, *ADAMTS13* was also identified as the responsible gene for hereditary TTP by linkage analysis.[19] ADAMTS-13 consists of 1,427 amino acid residues, containing an N-terminal signal peptide, a propeptide, a reprolysin-like metalloprotease domain, a disintegrin-like domain, a thrombospondin type-1 motif (TSP1), a cysteine-rich domain, a spacer domain, seven additional TSP1 repeats, and two CUB domains (Fig 1). Its mRNA is predominantly expressed in liver.[16,17,19,20]

Functional Properties of ADAMTS-13

The only known physiological substrate of ADAMTS-13 is VWF multimers, which play a pivotal role in platelet aggregation. ADAMTS-13 specifically cleaves the peptidyl bond between Y1605 and M1606 in the VWF A2 domain.[21-24] Systematic studies on the structure and function of ADAMTS-13, using recombinant ADAMTS-13 with progressive C-terminal truncations, determined the domains required for

From the National Cardiovascular Center Research Institute, Osaka, Japan.

Supported in part by grants-in-aid from the Ministry of Health, Labour, and Welfare of Japan, and from the Ministry of Education, Culture, Sports, Science, and Technology of Japan.

Address correspondence to Toshiyuki Miyata, PhD, National Cardiovascular Center Research Institute, 5-7-1 Fujishirodai, Suita, Osaka 565-8565, Japan.

0037-1963/04/4101-0002$30.00/0
doi:10.1053/j.seminhematol.2003.10.002

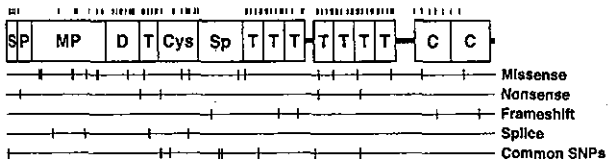

Figure 1. ADAMTS-13 mutations. The mutated sites responsible for hereditary TTP and common SNPs are shown below the domain structures of human ADAMTS-13. All cysteine residues are shown above. S, signal peptide; P, propeptide; MP, metalloprotease domain; D, disintegrin-like domain; T, TSP1 motif; Cys, cysteine-rich domain; Sp, spacer domain; C, CUB domain.

VWF cleavage.[25,26] Enzymatic analysis of these mutants showed that removal of the cysteine-rich/spacer domains caused loss of proteolytic activity towards VWF. The more C-terminal TSP1 and CUB domains were dispensable for VWF-cleaving activity, at least in vitro.

Thirty-three Mutations Responsible for TTP

To date, 33 mutations responsible for hereditary TTP have been identified in the *ADAMTS13* gene[19,27-30] (Table 1 and Fig 1). Five result in frameshift deletions or insertions and four are splice mutations. The remaining 24 mutations lead to codon changes, 19 of which are nonconservative missense and five of which are nonsense mutations. The mutated sites in *ADAMTS13* are distributed across many exons and introns throughout the gene, which spans approximately 37 kb on chromosome 9q34. The absence of clusters of mutations within the metalloprotease domain implies structural and functional importance of other regions.

Missense Mutations

Nineteen missense mutations have been identified: H96D, R102C, R193W, T196I, L232Q, S263C, R268P, P353L, R398H, C508Y, R528G, I673F, R692C, C908Y, C951G, C1024G, R1123C, C1213Y, and R1336W. Nine mutations are substitutions to/from cysteine residues, suggesting that disulfide-bond formation is important for proper conformation and function.

Among these, only six mutations were characterized by expression analysis.[27,31] We made mammalian expression plasmids for the R193W, R268P, C508Y, I673W, C908Y, and R1123C mutants, as well as wild-type ADAMTS-13, and then transfected them into cultured HeLa cells. A FLAG-tag sequence was added to the C terminus to aid in immunochemical detection. Transient expression of wild-type ADAMTS-13 produced a single immunoreactive band in culture medium, whereas none of the mutants were secreted, except for the R193W mutant, which was secreted at very low levels. Therefore, these six mutations must affect some aspect of the secretory pathway, possibly causing changes in protein folding and stability. The majority of the 19 identified missense mutations may cause secretory problems, similar to those in these five mutations.

Nonsense Mutations

Five nonsense mutations have been found: Q44X, W390X, Q449X, R910X, and R1034X. Among these, only one mutation, Q449X, was characterized by expression analysis.[26,27] The Q449X mutant was secreted efficiently like wild-type ADAMTS-13, but showed little cleavage activity towards VWF multimers.

As described above, the ADAMTS-13 spacer region is necessary for normal enzymatic activity. Since the W390X and Q449X mutants do not contain the spacer region, they would not possess VWF-cleaving activity, even if they are secreted. Alternatively, mRNAs derived from these nonsense mutant *ADAMTS13* genes may be destroyed by the nonsense-mediated decay (NMD) pathway (mRNA surveillance), which

Table 1. *ADAMTS13* Gene Mutations Responsible for Hereditary TTP

Exon/ Intron	Nucleotide	AA	Domain	Reference
Ex. 2	130C→T	Q44X	Propeptide	29
Ex. 3	286C→G	H96D	Metalloprotease	19
Ex. 3	304C→T	R102C	Metalloprotease	19
Int. 4	414+1G→A	Splice	Metalloprotease	31
Ex. 6	577C→T	R193W	Metalloprotease	31
Ex. 6	587C→T	T196I	Metalloprotease	19
Int. 6	686+1G→A	Splice	Metalloprotease	31
Ex. 7	695T→A	L232Q	Metalloprotease	28
Ex. 7	788C→G	S263C	Metalloprotease	28
Ex. 7	803G→C	R268P	Metalloprotease	27
Ex. 9	1058C→T	P353L	Disintegrin-like	28
Ex. 10	1169G→A	W390X	Tsp1-1	28
Ex. 10	1193G→A	R398H	Tsp1-1	19
Int. 10	1244+2T→G	Splice	Tsp1-1	31
Ex. 12	1345C→T	Q449X	Cysteine-rich	27
Ex. 13	1523G→A	C508Y	Cysteine-rich	27
Ex. 13	1582A→G	R528G	Cysteine-rich	19
Int. 13	1584+5G→A	Splice	Cysteine-rich	19
Ex. 15	1783delTT	Frameshift	Spacer	30
Ex. 17	2017A→T	I673F	Spacer	31
Ex. 17	2074C→T	R692C	Tsp1-2	19
Ex. 19	2376del26	Frameshift	Tsp1-3	19
Ex. 20	2549delAT	Frameshift	Tsp1-4	28
Ex. 21	2723G→A	C908Y	Tsp1-5	31
Ex. 21	2728C→T	R910X	Tsp1-5	28
Ex. 22	2851T→G	C951G	Tsp1-5	19
Ex. 24	3070T→G	C1024G	Tsp1-7	19
Ex. 24	3100A→T	R1034X	Tsp1-7	28
Ex. 25	3367C→T	R1123C	Tsp1-8	31
Ex. 26	3638G→A	C1213Y	CUB1	19
Ex. 27	3769insT	Frameshift	CUB1	19
Ex. 28	4006C→T	R1336W	CUB2	29
Ex. 29	4143insA	Frameshift	CUB2	28

Table 2. Mutated Alleles of Each Patient With Hereditary TTP

Patient	Allele 1	Allele 2	Reference
A1	R692C	R692C	9
A2	H96D	C951G	19
A3	R528G	Frameshift (3769insT)	19
A4	R398H	C1024G	19
A5	R102C	T196I	19
A6	Frameshift (2376del26)	C1213Y	19
A7	Splice (1584+5G→A)	ND	19
B1	R268P	C508Y	27
B2	Q449X	Q449X	27
C1	S263C	Frameshift (4143insA)	28
C2	P353L	R910X	28
C3	R1034X	Frameshift (4143insA)	28
C4	L232Q	L232Q	28
C5	W390X	Frameshift (2549delAT)	28
C6	P353L	Frameshift (4143insA)	28
C7	R910X	Frameshift (4143insA)	28
D1	Q44X	R1336W	29
E1	Frameshift (1783delTT)	Frameshift (1783delTT)	30
F1	Splice (414+1G→A)	Splice (414+1G→A)	31
F2	Splice (414+1G→A)	1673F	31
F3	1673F	C908Y	31
F4	R193W	Splice (1244+2T→G)	31
F5	Splice (686+1G→A)	R1123C	31

is one of the quality-control mechanisms that ensure high fidelity of gene expression. The NMD pathway destroys aberrant mRNAs that contain premature termination codons.[32,33] Therefore, ADAMTS-13 mutants with nonsense mutations may not be translated in vivo.

Frameshift Mutations

Five frameshift mutations have been identified: 1783delTT, 2376del26 (2376-2401del), 2549delAT, 3769insT, and 4143insA. If these mutated forms of ADAMTS-13 were to be translated, truncated mutants with aberrant C-terminal ends would be expressed. Each mutation replaces L595-T1427 with GGEDRRALCRGWEDEHLP, A793-T1427 with PALPCQVGGVRAQLMHISWWSRPGLGERDLCARGRWPGGSSD, D850-T1427 with GEAACP, L1258-T1427 with VGHDFQLQDQHAGGEAALRAARRWGAAAVWEPACS, or E1382-T1427 with REQPG, respectively. Some of these forms may not be secreted, and others may be secreted but dysfunctional. However, like the nonsense mutations described above, mRNAs with these frameshift mutations might be eliminated by gene expression quality-control systems.

Splice Mutations

Four splice mutations have been found: 414+1G→A, 686+1G→A, 1244+2T→G, and 1584+5G→A. The 414+1G→A (intron 4), 686+1G→A (intron 6), and 1244+2T→G (intron 10) mutations cause inconsistencies with the GT-AG rules of mRNA splicing. The 1584+5G→A (intron 13) mutation also alters the donor splice site from the consensus sequence. In fact, the effect of each of these mutations on mRNA splicing was examined experimentally. Total RNAs were isolated from patients' lymphoblasts or whole blood cells and used as templates for reverse-transcriptase polymerase chain reaction (RT-PCR). The data indicated that little or no normally spliced products were generated from the mutant alleles.[19,31]

Frequency of TTP-Causing Mutations

All 33 mutations were excluded as common sequence polymorphisms by screening a large panel of unaffected chromosomes. However, nine of these mutations occur on several occasions in 23 TTP patients (Table 2). Notably, this multiplicity occurs within the subjects of each investigator group. This suggests that *ADAMTS13* mutations may be specific to limited areas rather than be shared across the world. Specifically, Schneppenheim et al identified four alleles with the frameshift mutation 4143insA in seven unrelated German patients,[28] suggesting that the mutation is a relatively common polymorphism in areas as compared with other rare mutations.

Although most patients with hereditary TTP are compound heterozygotes at the *ADAMTS13* gene, some patients are homozygotes. Levy et al identified three patients with homozygous R692C mutations,

Table 3. Common Missense SNPs Identified in the *ADAMTS13* Gene

Exon	Nucleotide	AA	Domain	References
1	19C→T	R7W	Signal peptide	19,29
12	1342C→G	Q448E	Cysteine-rich	19,27,29
12	1423C→T	P475S	Cysteine-rich	27
16	1852C→G	P618A	Spacer	19,29
16	1874G→A	R625H	Spacer	19
18	2195C→T	A732V	Tsp1-2	19,29
21	2699C→T	A900V	Tsp1-5	19
24	3097G→A	A1033T	Tsp1-7	19

who all came from the same small village where the families lived for several generations.[19] We identified a homozygous patient with a Q449X mutation, whose two great-grandparents came from the same village in the northeastern region of the Japanese mainland at the end of the 19th century.[27] The patient with the homozygous 414+1G→A splice mutation had a family history of consanguineous marriage.[31] The patient with the homozygous L232Q mutation also likely came from a consanguineous pedigree, based on analysis of an intragenic haplotype.[28] The patient with the homozygous 1783delTT frameshift mutation was born to parents who were first cousins of Yemenite background.[30] Thus, all five homozygous mutations appear to be the progeny of some blood relationship.

Common Single-Nucleotide Polymorphisms

In all, eight missense mutations were reported as common single-nucleotide polymorphisms (SNPs)[19,27,29] (Table 3). In addition, Levy et al reported eight silent SNPs in eight exons and 10 SNPs in eight introns.[19] Thus far, no relationship between these SNPs and the development of TTP has been suspected.

The allele frequencies of R7W, Q448E, P475S, and P618A SNPs have been reported. We sequenced 364 Japanese subjects without TTP, and identified 125 heterozygotes and eight homozygotes of Q448E, and 35 heterozygotes and one homozygote of P475S. The allele frequencies were calculated to be 19% and 5%, respectively.[27] Since a 43% frequency of Q448E was also determined among 120 European alleles,[29] this SNP seems to be spread worldwide. In contrast, the P475S SNP was only reported by us. We sequenced 95 Caucasian subjects and found no alleles positive for the SNP (unpublished data, January 2003). Therefore, the P475S SNP may be localized to restricted areas around Japan. Antoine et al also reported the allele frequencies of R7W and P618A, as 10% and 9%, respectively.[29]

We prepared recombinant ADAMTS-13 with Q448E or P475S mutations and measured their cleavage activities toward VWF multimers.[27] The Q448E mutant showed normal activity, whereas the P475S mutant had a significantly reduced activity (~5% to 10% of wild type). The allele frequency of P475S is about 5%, as described above, suggesting that approximately 10% of the Japanese population are heterozygotes and may possess significantly reduced ADAMTS-13 activity. Theoretically, one in 400 Japanese may be P475S homozygotes, with quite low activity.

Sequencing Methods

We have performed *ADAMTS13* sequence analysis as described previously[27] with a slight modification. This analysis was carried out with the permission of ethics committees. Human genomic DNA was isolated from whole blood using the FlexiGene DNA kit (Qiagen, Hilden, Germany) or an automated nucleic acid isolation system, NA-3000 (Kurabo, Osaka, Japan). All exons of the *ADAMTS13* gene, including the intron-exon boundaries, were PCR-amplified with corresponding intronic primers (Table 4). Twenty-six primer sets were used. PCR was performed using HotStarTaq DNA polymerase (Qiagen) or the GC-RICH PCR system (Roche, Tokyo, Japan). For all exons, except 7 and 8, 10 μL of HotStarTaq Master Mix was added to 10 μL of water containing 50 ng of genomic DNA, 1 μmol/L forward primer, and 1 μmol/L reverse primer. For the amplification of exon 7, 0.4 μL of GC-RICH Enzyme Mix was added to 19.6 μL of water containing 50 ng of genomic DNA, 0.25 μmol/L forward primer, 0.25 μmol/L reverse primer, 0.2 mmol/L dNTP, and 4 μL of 5× GC-RICH PCR reaction buffer. For exon 8, 10 μL of HotStarTaq Master Mix was added to 10 μL of water containing 250 ng of genomic DNA, 4 μmol/L forward primer, 4 μmol/L reverse primer, and 5% dimethyl sulfoxide. The thermal cycle conditions for each reaction are summarized in Table 4. PCR products were purified using the QIAquick PCR Purification kit (Qiagen), and sequenced in both directions using a BigDye Terminator Kit (Applied Biosystems, Foster City, CA) and a 3700 DNA Analyzer (Applied Biosystems).

Future Issues

The coming sequence analysis of hereditary TTP patients will likely reveal still more *ADAMTS13* mutations. At present, it is difficult to define a correlation between each genotype and phenotype for TTP patients. Patients with hereditary TTP differ greatly in the age of onset and severity of symptoms. About half of hereditary TTP patients have their first acute episode during childhood, while the other half are

Table 4. Amplification of *ADAMTS13* Exons

Exon (bp)	Forward Primer	Reverse Primer	Product (bp)	PCR Step 1	PCR Step 2
1 (549)	GATTGCCAGGCCGTTTGTGAT	GCAAACCCCAAAGCTGATGTA	768	95°C/15 min	(94°C/20 s, 63°C/20 s, 72°C/45 s) × 40
2 (67)	CCTCGGTCTCCCCAAGTGTTA	GAACCCTGGCCTGGCTGGAAC	348	95°C/15 min	(94°C/20 s, 60°C/20 s, 72°C/45 s) × 35
3 (158)	GGTGGGGGTGACACGCAATGT	CCAGGGGAGGGAGGGAGAAGA	437	95°C/15 min	(94°C/20 s, 60°C/20 s, 72°C/45 s) × 35
4 (84)	TGTTTTCCTTGCGTTAGTTGG	GAGGATGGAGATGCGATGACT	382	95°C/15 min	(94°C/20 s, 60°C/20 s, 72°C/45 s) × 35
5-6 (125, 147)	AACAAACCGACCGCAGTCAGC	GGTTCCCCTGTCCTCACACCT	638	95°C/15 min	(94°C/20 s, 60°C/20 s, 72°C/45 s) × 35
7 (138)	GCTGGCGCTGCGGCACTAGGG	GTTGGACGGAGGGGTGGGTTG	399	95°C/3 min	(95°C/30 s, 64°C/30 s, 72°C/45 s) × 38
8 (163)	ACTCCTCCGTCCCGCCTCCTC	GCCCTCCCAGGACTAGCTACA	477	95°C/15 min	(94°C/20 s, 64°C/20 s, 72°C/30 s) × 40
9 (105)	GTGCAGAGTGTTGGCTGTGTC	CTCTGCCCCATACTGGTCCTG	334	95°C/15 min	(94°C/20 s, 60°C/20 s, 72°C/45 s) × 35
10-11 (152, 64)	TGAGGATGTTGGGGGACTCTC	CAAATGTGTCCTGGTGTGAAC	512	95°C/15 min	(94°C/20 s, 60°C/20 s, 72°C/45 s) × 35
12 (127)	TGAGGCCACACCCACATCTTG	ATGCCAGAGCCTGAACCACTT	366	95°C/15 min	(94°C/20 s, 60°C/20 s, 72°C/45 s) × 35
13 (149)	ATAGAAACCCTTGCCCCAGAT	ATCCTTTTCCCCAGCACCACT	390	95°C/15 min	(94°C/20 s, 63°C/20 s, 72°C/45 s) × 40
14 (121)	CAGGGCTGCAGAGTCATTGAG	GAAGGGTGGCGAAGTGGAAGA	358	95°C/15 min	(94°C/20 s, 60°C/20 s, 72°C/45 s) × 35
15 (81)	CTCCCTTTGTCTGTGGTGTGG	ACTATCAAGCCTGAGGGTGGT	279	95°C/15 min	(94°C/20 s, 60°C/20 s, 72°C/45 s) × 35
16 (182)	GGGACCCCGGGAAGGAGAGTC	GTAAGTGACCGCTGAATGAAT	393	95°C/15 min	(94°C/20 s, 60°C/20 s, 72°C/45 s) × 35
17-18 (136, 130)	GGCCAGGCTGGAGTGCTATGT	CAGAATGGGGGCACTCACAGA	770	95°C/15 min	(94°C/20 s, 63°C/20 s, 72°C/45 s) × 40
19 (186)	ACCAGCCTGTGATTCGGTTGT	AGGAACTCTGACAGCAGCACT	548	95°C/15 min	(94°C/20 s, 60°C/20 s, 72°C/45 s) × 35
20 (190)	CTCTTTGGGCTCCTGGATGTT	CAATGGGTGCTCCTCGTTCTC	386	95°C/15 min	(94°C/20 s, 60°C/20 s, 72°C/45 s) × 35
21 (121)	AAGGATACCCGCTGCGAGACC	AGCCAATCAACACCCACATTT	489	95°C/15 min	(94°C/20 s, 60°C/20 s, 72°C/45 s) × 35
22 (130)	CCATGCCGGCCTTATGTGCTA	TCTGGGTTGCAGTCCTCAAAG	439	95°C/15 min	(94°C/20 s, 60°C/20 s, 72°C/45 s) × 35
23 (183)	GGGGGCCTCCAGAAAGAGAAC	GTGTTGCCCAGGTTGGACTTG	476	95°C/15 min	(94°C/20 s, 60°C/20 s, 72°C/45 s) × 35
24 (205)	GGCTCAGTGGCTGCACTTTCC	TCCAGCGTCCCCAAACCTAAG	576	95°C/15 min	(94°C/20 s, 60°C/20 s, 72°C/45 s) × 35
25 (319)	GACAGGGACCCAGACTTGAAT	AAGTTACTTCCCCTTGATAGT	729	95°C/15 min	(94°C/20 s, 60°C/20 s, 72°C/45 s) × 35
26 (147)	CTGCATGTGCCCCCTCTTGCT	TGGGCACATCACTTAATCTCT	574	95°C/15 min	(94°C/20 s, 60°C/20 s, 72°C/45 s) × 35
27 (177)	GTGCATTCCCACCTGTAGTTT	TCCCTGGCACGTGCAGACTGA	583	95°C/15 min	(94°C/20 s, 60°C/20 s, 72°C/45 s) × 35
28 (185)	CCAGAGCCCAGAACATTTAGC	GCCACTATTTCACTCTTGTAG	581	95°C/15 min	(94°C/20 s, 60°C/20 s, 72°C/45 s) × 35
29 (412)	GTGTCCTTGGGGAAGTGATGT	GATTGGATTTTCTTCCTGGAT	757	95°C/15 min	(94°C/20 s, 60°C/20 s, 72°C/45 s) × 35

NOTE. All exons except exon 7 are amplified using HotStarTaq DNA polymerase. Exon 7 is amplified using GC-RICH PCR system. The reaction mixture for exon 8 contains 5% dimethyl sulfoxide.

affected in adulthood. Symptoms in adults often develop in association with stress of infection or pregnancy.[34] Genetic backgrounds other than *ADAMTS13* or environmental factors may be associated with the etiology of TTP.

From the viewpoint of clinical genetics, some problems still remain to be resolved. First, is the genetic variation in *ADAMTS13*, including common SNPs, associated with acquired TTP? Although the majority of TTP is the acquired type, with autoantibodies to ADAMTS-13, almost all subjects analyzed so far have had hereditary TTP. Sequence analysis of many patients with acquired TTP may help answer this question.

Second, are common SNPs that influence VWF-cleaving activity associated with other diseases? Although the almost complete loss of ADAMTS-13 activity results in TTP, the decreased activity may also be a risk factor for some thrombotic diseases, due to large circulating VWF multimers. In fact, a recent report suggested that levels of ADAMTS-13 activity are decreased in patients with coronary heart disease.[35] Common SNPs causing less than normal activity may also be linked to other disorders. The epidemiologic assessment of the P475S SNP will be important, at least in Japan.

Third, can VWF mutation be responsible for TTP? All hereditary TTP patients analyzed so far had mutations in *ADAMTS13*, and no *VWF* mutations were identified. Many mutations of *VWF* that enhance susceptibility to ADAMTS-13 and lead to the loss of large VWF multimers have been identified as the cause of type 2A von Willebrand disease. In contrast, no mutations conferring resistance against ADAMTS-13 proteolysis have been found. Such mutations might be lethal in the uterus. Analysis of genetically engineered animals may be useful to investigate this issue.

Fourth, do mutations causing deficiency of *THBS1*, which encodes thrombospondin-1, cause TTP? Two molecules are known that control the size of VWF multimers, ADAMTS-13 and thrombospondin-1. The latter is a trimeric glycoprotein that uncouples VWF multimers by reducing the disulfide-bonds that link individual subunits.[36,37] A combination of common genetic variations of *ADAMTS13*, *VWF*, and *THBS1* may be associated with TTP and other thrombotic diseases.

Additional Information

At the same time as the deadline for this manuscript, the 19th Congress of the International Society on Thrombosis and Haemostasis was held in Birmingham, UK. Eighteen additional mutations causing TTP were reported there by three research groups.[38-40] Reduced activity of some mutants was confirmed by expression analysis. The activities of recombinant ADAMTS-13 with common SNPs, R7W, P618A, A900V, and A1033T, were also measured.[41] The P475S SNP was also found in the Chinese population, but its allele frequency was remarkably lower than that in the Japanese population.[42]

References

1. Moschcowitz E: Hyaline thombrosis of the terminal arterioles and capillaries; a hitherto undescribed disease. Proc NY Pathol Soc 24:21-24, 1924
2. Kinoshita S, Yoshioka A, Park YD, Ishizashi H, Konno M, Funato M, et al: Upshaw-Schulman syndrome revisited: A concept of congenital thrombotic thrombocytopenic purpura. Int J Hematol 74:101-108, 2001
3. Fujimura Y, Titani K: Structure and function of von Willebrand factor, in Bloom AL, Forbes CD, Thomas DP, Tuddenham EGD (eds): Haemostasis and Thrombosis. New York, NY, Churchill Livingstone, 1994, pp 379-395
4. Furlan M: Von Willebrand factor: Molecular size and functional activity. Ann Hematol 72:341-348, 1996
5. Ruggeri ZM: von Willebrand factor. J Clin Invest 99:559-564, 1997
6. Sadler JE: Biochemistry and genetics of von Willebrand factor. Annu Rev Biochem 67:395-424, 1998
7. Chung DW, Fujikawa K: Processing of von Willebrand factor by ADAMTS-13. Biochemistry 41:11065-11070, 2002
8. Fujimura Y, Matsumoto M, Yagi H, Yoshioka A, Matsui T, Titani K: Von Willebrand factor-cleaving protease and Upshaw-Schulman syndrome. Int J Hematol 75:25-34, 2002
9. George JN, Sadler JE, Lämmle B: Platelets: Thrombotic thrombocytopenic purpura. Hematology (Am Soc Hematol Educ Program) 9:315-334, 2002
10. Zheng X, Majerus EM, Sadler JE: ADAMTS13 and TTP. Curr Opin Hematol 9:389-394, 2002
11. Tsai HM: Platelet activation and the formation of the platelet plug: Deficiency of ADAMTS13 causes thrombotic thrombocytopenic purpura. Arterioscler Thromb Vasc Biol 23:388-396, 2003
12. Furlan M, Robles R, Galbusera M, Remuzzi G, Kyrle PA, Brenner B, et al: von Willebrand factor-cleaving protease in thrombotic thrombocytopenic purpura and the hemolytic-uremic syndrome. N Engl J Med 339:1578-1584, 1998
13. Tsai HM, Lian EC: Antibodies to von Willebrand factor-cleaving protease in acute thrombotic thrombocytopenic purpura. N Engl J Med 339:1585-1594, 1998
14. Fujikawa K, Suzuki H, McMullen B, Chung D: Purification of human von Willebrand factor-cleaving protease and its identification as a new member of the metalloproteinase family. Blood 98:1662-1666, 2001
15. Gerritsen HE, Robles R, Lämmle B, Furlan M: Partial amino acid sequence of purified von Willebrand factor-cleaving protease. Blood 98:1654-1661, 2001
16. Soejima K, Mimura N, Hirashima M, Maeda H, Hamamoto T, Nakagaki T, et al: A novel human metalloprotease synthesized in the liver and secreted into the blood: Possibly, the von Willebrand factor-cleaving protease? J Biochem 130:475-480, 2001
17. Zheng X, Chung D, Takayama TK, Majerus EM, Sadler JE, Fujikawa K: Structure of von Willebrand factor-cleaving protease (ADAMTS13), a metalloprotease involved in thrombotic thrombocytopenic purpura. J Biol Chem 276:41059-41063, 2001

18. Plaimauer B, Zimmermann K, Volkel D, Antoine G, Kerschbaumer R, Jenab P, et al: Cloning, expression, and functional characterization of the von Willebrand factor-cleaving protease (ADAMTS13). Blood 100:3626-3632, 2002
19. Levy GG, Nichols WC, Lian EC, Foroud T, McClintick JN, McGee BM, et al: Mutations in a member of the ADAMTS gene family cause thrombotic thrombocytopenic purpura. Nature 413:488-494, 2001
20. Cal S, Obaya AJ, Llamazares M, Garabaya C, Quesada V, López-Otín C: Cloning, expression analysis, and structural characterization of seven novel human ADAMTSs, a family of metalloproteinases with disintegrin and thrombospondin-1 domains. Gene 283:49-62, 2002
21. Dent JA, Berkowitz SD, Ware J, Kasper CK, Ruggeri ZM: Identification of a cleavage site directing the immunochemical detection of molecular abnormalities in type IIA von Willebrand factor. Proc Natl Acad Sci USA 87:6306-6310, 1990
22. Tsai HM, Sussman II, Nagel RL: Shear stress enhances the proteolysis of von Willebrand factor in normal plasma. Blood 83:2171-2179, 1994
23. Furlan M, Robles R, Lämmle B: Partial purification and characterization of a protease from human plasma cleaving von Willebrand factor to fragments produced by in vivo proteolysis. Blood 87:4223-4234, 1996
24. Tsai HM: Physiologic cleavage of von Willebrand factor by a plasma protease is dependent on its conformation and requires calcium ion. Blood 87:4235-4244, 1996
25. Zheng X, Nishio K, Majerus EM, Sadler JE: Cleavage of von Willebrand factor requires the spacer domain of the metalloprotease ADAMTS13. J Biol Chem 278:30136-30141, 2003
26. Soejima K, Matsumoto M, Kokame K, Yagi H, Ishizashi H, Maeda H, et al: ADAMTS-13 cysteine-rich/spacer domains are functionally essential for von Willebrand factor cleavage. Blood 102:3232-3237, 2003
27. Kokame K, Matsumoto M, Soejima K, Yagi H, Ishizashi H, Funato M, et al: Mutations and common polymorphisms in ADAMTS13 gene responsible for von Willebrand factor-cleaving protease activity. Proc Natl Acad Sci USA 99:11902-11907, 2002
28. Schneppenheim R, Budde U, Oyen F, Angerhaus D, Aumann V, Drewke E, et al: von Willebrand factor cleaving protease and ADAMTS13 mutations in childhood TTP. Blood 101: 1845-1850, 2003
29. Antoine G, Zimmermann K, Plaimauer B, Grillowitzer M, Studt JD, Lämmle B, et al: ADAMTS13 gene defects in two brothers with constitutional thrombotic thrombocytopenic purpura and normalization of von Willebrand factor-cleaving protease activity by recombinant human ADAMTS13. Br J Haematol 120:821-824, 2003
30. Savasan S, Lee SK, Ginsburg D, Tsai HM: ADAMTS13 gene mutation in congenital thrombotic thrombocytopenic purpura with previously reported normal VWF cleaving protease activity. Blood 101:4449-4451, 2003
31. Matsumoto M, Kokame K, Soejima K, Miura M, Hayashi S, Fujii Y, et al: Molecular characterization of ADAMTS13 gene mutations in Japanese patients with Upshaw-Schulman syndrome. Blood (in press)
32. Wagner E, Lykke-Andersen J: mRNA surveillance: the perfect persist. J Cell Sci 115:3033-3038, 2002
33. Wilkinson MF, Shyu AB: RNA surveillance by nuclear scanning? Nat Cell Biol 4:E144-147, 2002
34. Furlan M, Lämmle B: Aetiology and pathogenesis of thrombotic thrombocytopenic purpura and haemolytic uraemic syndrome: The role of von Willebrand factor-cleaving protease. Best Pract Res Clin Haematol 14:437-454, 2001
35. Yoo G, Blomback M, Schenck-Gustafsson K, He S: Decreased levels of von Willebrand factor-cleaving protease in coronary heart disease and thrombotic thrombocytopenic purpura: Study of a simplified method for assaying the enzyme activity based on ristocetin-induced platelet aggregation. Br J Haematol 121:123-129, 2003
36. Xie L, Chesterman CN, Hogg PJ: Control of von Willebrand factor multimer size by thrombospondin-1. J Exp Med 193: 1341-1349, 2001
37. Pimanda JE, Annis DS, Raftery M, Mosher DF, Chesterman CN, Hogg PJ: The von Willebrand factor-reducing activity of thrombospondin-1 is located in the calcium-binding/C-terminal sequence and requires a free thiol at position 974. Blood 100:2832-2838, 2002
38. Motto D, Levy G, Mcgee B, Tsai H, Ginsburg D: ADAMTS13 mutations identified in familial TTP patients result in loss of VWF-cleaving protease activity. J Thromb Haemost 1:OC115, 2003 (suppl 1)
39. Schneppenheim R, Angerhaus D, Mainusch K, Obser T, Oyen F, Budde U: Comparative expression of recombinant wild-type and mutant von Willebrand factor cleaving protease ADAMTS13. J Thromb Haemost 1:OC117, 2003 (suppl 1)
40. Veyradier A, Lavergne JM, Obert B, Ribba AS, Fressinaud E, Loirat C, et al: Identification of seven new candidate mutations of ADAMTS13 gene in four French families related to congenital thrombotic thrombocytopenic purpura. J Thromb Haemost 1:P0310, 2003 (suppl 1)
41. Peyvandi F, Lavoretano S, Canciani MT, Mannucci PM: In vitro expression study of four single nucleotide polymorphisms in the ADAMTS13 gene. J Thromb Haemost 1:P0325, 2003 (suppl 1)
42. Gao WQ, Wang ZY, Bai X, Ruan C: The frequency of P475S polymorphism in von Willebrand factor-cleaving protease among Chinese population and its relevance to arterial thrombotic disorders. J Thromb Haemost 1:P0376, 2003 (suppl 1)

Molecular characterization of *ADAMTS13* gene mutations in Japanese patients with Upshaw-Schulman syndrome

Masanori Matsumoto, Koichi Kokame, Kenji Soejima, Masayoshi Miura, Syuhei Hayashi, Yasuhiko Fujii, Asayuki Iwai, Etsuro Ito, Yoichiro Tsuji, Mayuko Takeda-Shitaka, Mitsuo Iwadate, Hideaki Umeyama, Hideo Yagi, Hiromichi Ishizashi, Fumiaki Banno, Tomohiro Nakagaki, Toshiyuki Miyata, and Yoshihiro Fujimura

We report here 7 new mutations in the *ADAMTS13* gene responsible for Upshaw-Schulman syndrome (USS), a catastrophic phenotype of congenital thrombotic thrombocytopenic purpura, by analyzing 5 Japanese families. There were 3 mutations that occurred at exon-intron boundaries: 414+1G>A at intron 4, 686+1G>A at intron 6, and 1244+2T>G at intron 10 (numbered from the A of the initiation Met codon), and we confirmed that 2 of these mutations produced aberrantly spliced messenger RNAs (mRNAs). The remaining 4 mutations were missense mutations: R193W, I673F, C908Y, and R1123C. In expression experiments using HeLa cells, all mutants showed no or a marginal secretion of ADAMTS13. Taken together with the findings in our recent report we determined the responsible mutations in a total of 7 Japanese patients with USS with a uniform clinical picture of severe neonatal hyperbilirubinemia, and in their family members, based on *ADAMTS13* gene analysis. Of these patients, 2 were homozygotes and 5 were compound heterozygotes. The parents of one homozygote were related (cousins), while those of the other were not. Molecular models of the metalloprotease, fifth domain of thrombospondin 1 (Tsp1-5), and Tsp1-8 domains of ADAMTS13 suggest that the missense mutations could cause structural defects in the mutants. (Blood. 2004;103:1305-1310)

Introduction

Thrombotic thrombocytopenic purpura (TTP) is a life-threatening generalized disorder, and its diagnosis is made according to the criteria of Moschcowitz's pentad[1]: thrombocytopenia, microangiopathic hemolytic anemia (MAHA), fluctuating neurologic signs, renal failure, and fever. These criteria, however, are almost undistinguishable from those of hemolytic-uremic syndrome (HUS) with Gasser's triad[2]; MAHA, thrombocytopenia, and renal insufficiency. Thus, the comprehensive term "TTP/HUS" or "thrombotic microangiopathy"[3] has frequently been used in clinical practice.

Recent advances in elucidating the proteolytic processing of plasma von Willebrand factor (VWF) multimers have established assays for the activity of VWF-cleaving protease and its inhibitor (autoantibody).[4-7] These assays have largely made it possible to distinguish TTP from HUS, because the former has defective VWF-cleaving activity, whereas the latter has VWF-cleaving activity.[6,7] Studies by several groups of investigators have led to the identification of this enzyme as a new metalloprotease belonging to the ADAMTS (a disintegrinlike and metalloprotease with thrombospondin type 1 motif) family, which has been designated ADAMTS13.[8-12] This enzyme is produced in the liver.[10-12] The deduced amino acid residue number is 1427, and the gene contains 29 exons and is located on chromosome 9q34.[10-12]

Upshaw-Schulman syndrome (USS) was originally reported as a disease complex with repeated episodes of thrombocytopenia and hemolytic anemia that quickly respond to infusions of fresh frozen plasma (FFP).[13-16] Clinical signs often develop in the patients during the newborn period or early infancy. In fact, the earliest and most frequently encountered clinical manifestation is severe hyperbilirubinemia with negative Coombs test soon after birth, which requires exchange blood transfusions. Pediatric hematologists have long been more familiar with this disease than general physicians, but this diagnostic name appears to be lacking or ignored in most medical textbooks because of its uncertain clinical entity. Thus, a variety of alternative nomenclatures has been given to this disease, such as chronic relapsing TTP, congenital MAHA, and familial TTP/HUS.

Under these circumstances, the report of Furlan et al[17] in 1997 showing that 4 cases of chronic relapsing TTP lacked ADAMTS13 activity was notable. Of these cases, 2 were siblings with a

From the Departments of Blood Transfusion Medicine and Health Science, Nara Medical University, Kashihara, Japan; the National Cardiovascular Center Research Institute, Suita, Japan; the First Research Department, the Chemo-Sero-Therapeutic Research Institute, Kumamoto, Japan; the Department of Pediatrics, Toyama City Hospital, Toyama, Japan; the Department of Pediatrics, Fukui Red Cross Hospital, Fukui, Japan; the Department of Blood Transfusion Medicine, Yamaguchi University School of Medicine, Ube, Japan; the Department of Pediatrics, Kagawa Children's Hospital, Zentsuji, Japan; the Department of Pediatrics, Hirosaki University School of Medicine, Hirosaki, Japan; the Department of Pediatrics, Tokyo Medical and Dental University, Tokyo, Japan; and the School of Pharmaceutical Sciences, Kitasato University, Tokyo, Japan.

Submitted June 12, 2003; accepted September 29, 2003. Prepublished online as *Blood* First Edition Paper, October 16, 2003; DOI 10.1182/blood-2003-06-1796.

Supported in part by Grants-in-Aid for Scientific Research grant from the Japanese Ministry of Education, Culture, Sports, Science, and Technology (M. Matsumoto, K.K., T.M. and Y. Fujimura); from the Ministry of Health and Welfare of Japan for Blood Coagulation Abnormalities H14-02 (T.M. and Y. Fujimura); and from the Program for Promotion of Fundamental Studies in Health Sciences of the Organization for Pharmaceutical Safety and Research of Japan (T.M. and K.K.).

M. Matsumoto and K.K. contributed equally to this work.

Reprints: Yoshihiro Fujimura, Department of Blood Transfusion Medicine, Nara Medical University, Shijyo-cho 840, Kashihara city, Nara 634-8522, Japan; e-mail: yfujimur@naramed-u.ac.jp.

The publication costs of this article were defrayed in part by page charge payment. Therefore, and solely to indicate this fact, this article is hereby marked "advertisement" in accordance with 18 U.S.C. section 1734.

consistent deficiency of the enzyme activity, suggesting that they had an inheritable form, whereas the other 2 were unrelated and apparently had an acquired form. Since then, there have been several reports on TTP/HUS associated with congenital deficiency of ADAMTS13 activity, and, accordingly, the diagnostic name of USS has been re-evaluated and has gained a position as an independent disease entity. Usually, parents of USS patients have reduced plasma ADAMTS13 activity, roughly half of the normal control level, indicating that they are asymptomatic carriers.[15] Among them, one father detected in our laboratory was particularly interesting because he had an extremely low level of plasma ADAMTS13 activity, 4.5% to 7% of the normal control level on 3 different occasions, but so far, at the age of 36, he has no apparent clinical signs.[15] The unusually low level of ADAMTS13 activity in this man was further confirmed by both genetic and biochemical analyses,[18] that is, he was compound heterozygote, R268P/P475S. In expression analysis, the R268P mutant was not secreted from the cells, but the P475S mutant was secreted normally and showed low but significant activity. The P475S mutation is prevalent in the Japanese population (heterozygosity ~ 10%). Thus, the discovery of new *ADAMTS13* mutations in different countries or races appears to be very important for the analysis of a potential linkage with other thrombotic generic risks.

Here, we identified 7 new mutations in the *ADAMTS13* gene responsible for USS by analyzing 5 patients and 16 relatives belonging to 5 different families from widely separated regions in Japan. All the patients had an episode of severe hyperbilirubinemia during the newborn period, and received exchange blood transfusions, except for one. Furthermore, structural changes of the mutant ADAMTS13 molecules associated with impaired enzyme activity were predicted using a homology modeling method.

Patients, materials, and methods

Families A to G with USS

Families C to G are shown in Figure 1.

Families A and B. There were 2 USS probands, A and B, belonging to different families described and characterized in detail in a recent publication.[18]

Family C. Proband C is a male born in Fukui in 1972 whose history during childhood was reported in 1984.[19] His parents are cousins. His father died of cerebral infarction at 63 years of age, and the third brother died of melena soon after birth. His mother and 2 other brothers have no thrombotic or hemorrhagic signs. Proband C showed hyperbilirubinemia during the newborn period, and he received phototherapy for 3 days without exchange blood transfusion. Thereafter, he had repeated episodes of thrombocytopenia and hemolytic anemia, and he has received prophylactic infusion of 2 units (160 mL) of FFP every 2 to 4 weeks since he was 8 years old. However, he has gradually developed chronic nephritis and was required to receive continuous ambulatory peritoneal dialysis starting in March 1995. Because of repeated peritonitis associated with continuous ambulatory peritoneal dialysis, however, his therapy for renal insufficiency was completely switched to hemodialysis starting in May 1999.

Family D. Proband D is a female born in Yamaguchi in 1978 whose history until the age of 4 years was reported in 1982.[20] Her parents are unrelated. She had an episode of severe hyperbilirubinemia soon after birth that required 2 exchange blood transfusions. Since 4 years of age, she received 1 unit (80 mL) of FFP every 3 weeks until the age of 21 years. Under this treatment regimen, however, her renal function test, including serum creatinine level, was getting worse, and therefore the volume of FFP infused was increased stepwise. She now receives 5 units (400 mL) of FFP infusion every 2 weeks for prophylaxis.

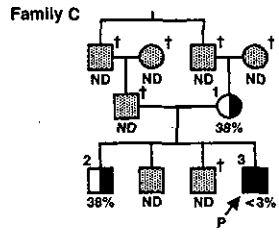

	414+1G
C-1	G/A
C-2	G/A
C-3	A/A

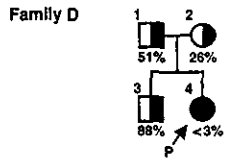

	414+1G	Ile673	Haplotype
D-1	G/G	I/F	GI/GF
D-2	G/A	I/I	GI/AI
D-3	G/A	I/I	GI/AI
D-4	G/A	I/F	GF/AI

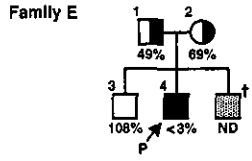

	Ile673	Cys908	Haplotype
E-1	I/F	C/C	IC/FC
E-2	I/I	C/Y	IC/IY
E-3	I/I	C/C	IC/IC
E-4	I/F	C/Y	IY/FC

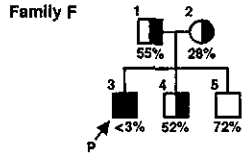

	Arg193	1244+2T	Haplotype
F-1	R/W	T/T	RT/WT
F-2	R/R	T/G	RT/RG
F-3	R/W	T/G	RG/WT
F-4	R/R	T/G	RT/RG
F-5	R/R	T/T	RT/RT

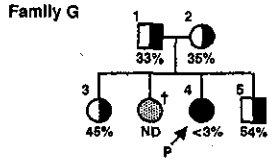

	686+1G	Arg1123	Haplotype
G-1	G/G	R/C	GR/GC
G-2	G/A	R/R	GR/AR
G-3	G/A	R/R	GR/AR
G-4	G/A	R/C	GC/AR
G-5	G/G	R/C	GR/GC

Figure 1. Pedigree and haplotypes of patient families. Squares and circles indicate males and females, respectively. Closed circles and squares with arrows with a P indicate probands. The half-closed circles and squares represent asymptomatic carriers. The cross indicates deceased. The ADAMTS13 activity is shown as a percentage of the normal control. ND indicates not determined. Mutations found in the *ADAMTS13* gene are shown as one-letter amino acid abbreviations numbered from the initial Met or as nucleotides numbered from the A of the translation initiation Met codon.

Family E. Proband E is a male born in Kagawa in 1985. He is the second child of unrelated parents. His younger brother with Down syndrome died of an unknown cause soon after birth. His parents and elder brother are apparently healthy. This proband developed severe hyperbilirubinemia and thrombocytopenia in the next day after birth. He received 2 exchange blood transfusions on the second day of life, resulting in excellent clinical improvement. At 5 years of age, he had an episode of thrombocytopenia and hemolytic anemia. Such clinical manifestations quickly improved after 2 plasma exchanges, together with the correction of abnormal laboratory test results that confirmed a clinical diagnosis of USS. After that, he receives 2 to 3 units (160-240 mL) of FFP infusion upon episodes of thrombocytopenia and hemolytic anemia.

Family F. Proband F is a male born in Aomori in 1993. He is the first child of unrelated parents. His parents and brothers are all apparently healthy. Soon after birth, this proband developed severe hyperbilirubinemia and received 2 exchange blood transfusions. At 10 months after birth, he had generalized petechiae with hemolytic anemia and thrombocytopenia. Therefore, he was once diagnosed with idiopathic thrombocytopenic purpura. At 2 ½ years of age, he received 1 unit (80 mL) of FFP infusion for the aforementioned clinical signs, which dramatically improved both his clinical and laboratory findings, resulting in a clinical diagnosis of USS. Now, he receives 1 unit of FFP infusion for each of his occasional hemolytic crises.

Family G. Proband G is a female born in Tokyo in 1987. She is the third child of unrelated parents. One elder sister had an episode of severe

hyperbilirubinemia soon after birth and received exchange blood transfusion. She died of intracranial bleeding after a traffic accident at 8 years old. Her parents, remaining elder sister, and brother are all apparently healthy. Soon after birth the proband developed severe hyperbilirubinemia and received exchange blood transfusion. Thereafter, she had repeated episodes of thrombocytopenia and hemolytic anemia that were quickly improved by FFP infusion. Finally, at 14 years of age, she was clinically diagnosed with USS. Now, she receives 10 mL/kg FFP infusion for each of her occasional hemolytic crises.

Assays of ADAMTS13 activity

Plasma ADAMTS13 activity was assayed by the method of Furlan et al[4,6] based on VWF multimer analysis, with a slight modification as described.[15] The ADAMTS13 activity of pooled normal plasma was defined as 100%. The normal range of ADAMTS13 activity (n = 60; 30 women and 30 men, 20-39 years of age) was 102 ± 23% (mean ± 1 SD).[21]

Sequencing of the *ADAMTS13* gene

All DNA experiments were performed with the permission of the ethics committees of both the sample-collecting hospital and the gene-analyzing institute. Amplification and sequencing of the 29 exons of the *ADAMTS13* gene were performed as recently described.[18]

Transient expression of ADAMTS13

Polymerase chain reaction (PCR)–based mutagenesis was performed for the construction of ADAMTS13 mutants as recently reported.[18] The mutant cDNA was cloned into mammalian expression vector, pCAGG.[22] The DNA sequence of all inserts was confirmed by DNA sequencing.

Each of the expression vectors was transfected into HeLa cells using FuGENE6 (Roche Molecular Biochemicals, Indianapolis, IN), according to the manufacturer's instructions. Briefly, HeLa cells were cultured in Dulbecco modified Eagle medium (Invitrogen, Carlsbad, CA) containing 10% fetal bovine serum (Invitrogen) in humidified air with 5% CO_2 at 37°C. Of each expression plasmid, 5 μg was transfected into subconfluent cells in 90-mm dishes. After 4 to 6 hours of incubation, the medium was changed to 4 mL serum-free OPTI-MEM I (Invitrogen), and the cultures were incubated for 44 hours. The media were collected and the culture media were concentrated to one tenth the original volume. The cells were washed with phosphate-buffered saline, pH 7.4, and lysed with 300 μL sodium dodecyl sulfate (SDS) sample buffer (10 mM Tris [tris(hydroxymethyl)aminomethane]–HCl/2% SDS/50 mM dithiothreitol/10 mM ethylenediaminetetraacetic acid/0.02% bromophenol blue/6% glycerol, pH 6.8).

Western blot analysis

The media and cell lysates were first separated by SDS–polyacrylamide gel electrophoresis and then transferred to a polyvinylidene difluoride membrane (BioRad, Hercules, CA). After blocking with 3% skim milk, the membrane was incubated with 1 μg/mL anti-FLAG (fludarabine, cytarabine, and granulocyte colony-stimulating factor) M2 monoclonal antibody (Sigma, St Louis, MO) and then 0.1 μg/mL peroxidase-labeled goat antimouse immunoglobulin G (Kirkegaard & Perry Laboratories, Gaithersburg, MD). Luminographic detection was performed using the Western Lighting Chemiluminescence Reagent (PerkinElmer Life Sciences, Shelton, CT) and detected using an image analyzer LAS 1000 plus (Fujifilm, Tokyo, Japan).

Reverse-transcription PCR

To evaluate the transcription products of the gene with a single nucleotide mutation in introns 4 and 10, we performed reverse transcription (RT)–PCR on mRNA using primers corresponding to the respective exons. RT-PCR for intron 4 using sense primer GGGCAGAACTGCTTCGGGACC (exon 4) and antisense primer AGCATGGCCAGGATCCGTGTC (exon 5) yields a 185–base pair (bp) band from the normally spliced transcript or a 510-bp band from the unspliced transcript. RT-PCR for intron 10 using sense primer GGGTCCCCGAAGTCCTTGCTC (exon 10) and antisense primer AGGTCAGCACCAACACATGCA (exon 11) yields a 115-bp band from the spliced transcript or a 226-bp band from the unspliced transcript. The mRNAs were prepared using a PAXgene Blood RNA system (Qiagen, Valencia, CA), and RT-PCR was performed using Qiagen OneStep RT-PCR (Qiagen).

Construction of 3-dimensional models of metalloprotease, Tsp1-5, and Tsp1-8 domains of ADAMTS13

Model structures of the wild-type (WT) metalloprotease domain, and fifth and eighth domains of thrombospondin 1 (Tsp1-5 and Tsp1-8 domains) were constructed based on homology modeling methods. Searching for the reference proteins and sequence alignments was performed using position-specific iterated (PSI)–BLAST.[23] The reference proteins were adamalysin II (PDB[24] ID: 4AIG[25]) for the metalloprotease domain and thrombospondin-1 type 1 repeats (PDB ID: 1LSL[26]) for Tsp1-5 and Tsp1-8 domains. The sequence alignments produced using PSI-BLAST were manually adjusted taking biologically important regions and secondary structure into consideration using the CHIMERA modeling system.[27,28] The model structures were constructed using the fully automatic modeling system FAMS[29,30] based on each alignment.

Results

ADAMTS13 activity and ADAMTS13 inhibitor in patients with USS and their families

The family pedigrees of 5 patients and their ADAMTS13 activity are shown in Figure 1. The plasma ADAMTS13 activities of all probands were less than 3% of the normal control value. The low activity (<3%) of ADAMTS13 in the proband was confirmed using the plasmas of at least 2 different occasions, with an interval of more than 6 months. The ADAMTS13 activity, which was less than 3% of the normal, of 2 other USS patients A and B in 2 different families was described in our previous paper.[17] Neither the patients' nor their relatives' plasmas contained detectable inhibitor of ADAMTS13 activity (<0.5 Bethesda unit/mL).

The earliest uniform clinical picture of these 7 patients was severe-to-moderate hyperbilirubinemia during the newborn period that required exchange blood transfusion, except in one case (patient C), who was treated with phototherapy. After the clinical diagnosis of USS was made, all patients were treated with a prophylactic infusion of 5 to 10 mL of FFP/kg at 2- to 3-week intervals or with FFP infusion when they had clinical manifestations.

ADAMTS13 gene mutations in patients with USS and their families

We analyzed the *ADAMTS13* gene in 5 patients with USS and 21 of their family members by PCR amplification and sequencing of the 29 exons of the gene. Single-nucleotide mutations at 12 sites were identified (Table 1). There were 4 silent mutations identified: 420T>C, 1716G>A, 2280C>T, and 4221C>A, and all of these mutations have been reported as single nucleotide polymorphisms (SNPs).[12,18] We identified 8 additional mutations in the 5 families. Of 8 mutations, 5 found in the exons were missense mutations: 577C>T (R193W), 1342C>G (Q448E), 2017A>T (I673F), 2723G>A (C908Y), and 3367C>T (R1123C). Of these, 1342C>G (Q448E) has been reported as an SNP.[12,18] The remaining 3 mutations were found in introns at +1 or +2 nucleotides from the exon-intron boundary, and these mutations in introns appeared to render the gene unable to produce a normally spliced transcript.

To investigate the frequencies of the 7 mutations newly identified in this report, we performed sequencing of exons 4, 6, 10, 17, 21, and 25 of the *ADAMTS13* gene in genomic DNAs isolated

Table 1. *ADAMTS13* mutations in 5 USS families

Exon	Family	Nucleotide	Amino acid
Intron 4	C, D	414+1G>A	Splice
5	F	420T>C*	Silent
6	F	577C>T	R193W
Intron 6	G	686+1G>A	Splice
Intron 10	F	1244+2T>G	Splice
12	F, G	1342C>G*	Q448E
15	F, G	1716G>A*	Silent
17	D, E	2017A>T	I673F
19	D, E, F, G	2280C>T*	Silent
21	E	2723G>A	C908Y
25	G	3367C>T	R1123C
29	F, G	4221C>A*	Silent

*Reported by Levy et al[12] and Kokame et al.[19]

from 96 Japanese individuals without TTP. They were all patients of the Division of Hypertension and Nephrology at the National Cardiovascular Center (Suita, Japan). None of these 7 mutations appeared in this panel, indicating that they were rare (<1% heterozygosity) in the Japanese population.

Expression of rADAMTS13 mutants

To determine the effects of the newly identified mutations, WT and mutant forms of recombinant ADAMTS13 (rADAMTS13) were transiently expressed in HeLa cells. The expression of WT rADAMTS13 produced a single immunoreactive band with a molecular mass of about 230 kDa in the culture medium (Figure 2, top). The band was not detected in the medium of untransfected cells. In the culture medium of cells expressing the R193W mutant, a weak band was detected with the same size as WT. The expression level of the R193W mutant was roughly estimated as one fourth of WT by comparing their chemiluminescent intensities on Western blot. On the other hand, no bands were detected for the I673F, C908Y, and R1123C mutants, although these mutants were synthesized within the cells (Figure 2, bottom). These results clearly indicated that these mutants are not secreted normally.

The enzymatic activity of rADAMTS13 was determined by analyzing the degradation of VWF multimers.[18] In the medium of untransfected cells, the ladders of VWF multimers extended into the high-molecular-weight area (Figure 3, untransfected), indicating the lack of ADAMTS13 activity in the medium. In contrast, the ladder diminished after incubation with the medium of transfected cells expressing WT rADAMTS13, indicating that WT has ADAMTS13 activity. This activity was also observed in the 1:4- and

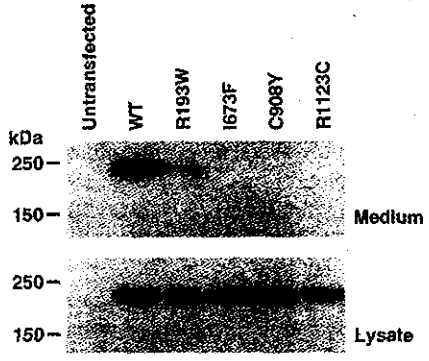

Figure 2. Expression of rADAMTS13. The wild-type (WT) rADAMTS13 and mutants with C-terminal FLAG-tag were transiently expressed in HeLa cells. The culture media (top) and cell lysates (bottom) were analyzed by Western blotting with an anti-FLAG antibody. The sizes of protein standards are indicated at the left.

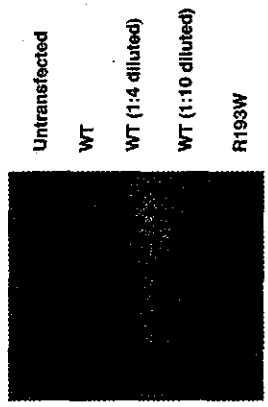

Figure 3. Cleavage of VWF multimer by rADAMTS13. The rADAMTS13 activity was measured by degradation of VWF multimers. The culture media of untransfected, WT, and the R193W mutant were incubated with purified VWF. The multimeric state of VWF was determined by Western blot analysis after SDS–agarose gel electrophoresis.The 1:4 diluted WT medium contained the enzyme amount roughly equivalent to the medium of the R193W mutant.

1:10-diluted WT. As for the R193W mutant, no enzymatic activity was observed (Figure 3), indicating that the R193W mutant had little activity.

Aberrant splicing caused by mutations at exon-intron boundary

To test the effects of the mutations in introns 4 and 10, we performed RT-PCR using exon primers. Since no bands corresponding to the RT-PCR products were detected without the reverse-transcription reaction in normal control samples, the possibility that bands were generated due to the contaminating genomic DNA was excluded (Figure 4, lane N(-RT)).

For the 414+1G>A mutation in intron 4, we examined mRNA from 6 individuals: healthy control (N), C-3 (homozygote for the mutation), D-1 (no mutation), and D-2 to D-4 (heterozygotes) (Figure 4, top). In N and D-1, only one band of 185 bp corresponding to the normally spliced product was detected. In D-2 to D-4, a 510-bp band corresponding to unspliced transcript was found together with the 185-bp band derived from the spliced transcript. In contrast, in C-3, only one band of 510 bp was found. Thus, it was clear that the mutation 414+1G>A abolished the splicing at the exon 4–intron 4 boundary.

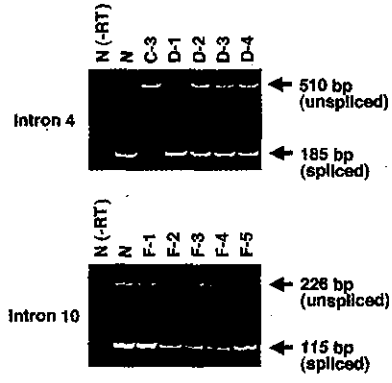

Figure 4. Effects of intronic mutations on mRNA splicing. To evaluate the products of genes with a single splice mutation in intron 4 (top) or intron 10 (bottom), we performed RT-PCR on mRNA using primers corresponding to these exons. RT-PCR for intron 4 yielded a 185-bp band from the normally spliced transcript and a 510-bp band from the unspliced transcript. RT-PCR for intron 10 yielded a 115-bp band from the spliced transcript and a 226-bp band from the unspliced transcript.

For the 1244+2T>G mutation in intron 10, we similarly performed RT-PCR on mRNA from 6 individuals: N, F-1 and F-5 (no mutation), and F-2 to F-4 (heterozygotes) (Figure 4, bottom). In this experiment, we were unable to obtain a sample of a homozygote for the mutation because the proband with this mutation was compound heterozygote. As a result, the product from all 6 individuals had 2 bands of 115 bp derived from the spliced transcript and 226 bp derived from the unspliced transcript. However, it is clear that the intensity of the 115-bp band of F-1 and F-5 was much denser than that of the 226-bp band. In contrast, the intensity of the 115-bp band of F-2 to F-4 was much weaker than that of N, F-1, and F-5. Based on these results, intron 10 appears to be not completely spliced even in healthy individuals, suggesting that in healthy individuals alternative splicing occurred at exon 10–intron 10 boundary or the splicing of this boundary had low efficiency. Furthermore, the transcripts of heterozygous individuals are likely to be less spliced than those of healthy individuals. Thus, the mutation of 1244+2T>G abolishes splicing at the exon-intron boundary.

Molecular modeling of the metalloprotease and Tsp1 domains of ADAMTS13

We constructed 3-dimensional molecular models of the metalloprotease and Tsp1 domains in which the mutations were identified. There are 2 missense mutations located in the metalloprotease domain: R193W identified in the present study and R268P identified in our previous study.[18] The R193W mutation is located close to the active site. Even if the mutant protein is secreted, the mutation is predicted to disturb the activity, as shown in Figures 2-3. The R268P mutation is located in the middle of an α-helix. It is well known that proline is an α-helix breaker. Therefore, it can be predicted that the R268P substitution would cause a secretion defect due to the disruption of one of the α-helices in the molecule.

The C908Y and R1123C mutations are present in the Tsp1-5 and Tsp1-8 domains, respectively (Figure 5B and 5C, respectively). The C908Y mutation may disrupt a potential disulfide bond and the R1123C mutation may create the mixed disulfide bond; both of them could disrupt the proper conformation of the enzyme, leading to the secretion defect.

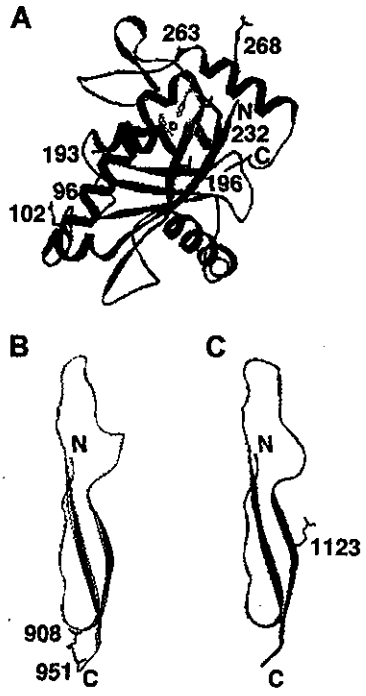

Figure 5. Shown are 3-dimensional models of metalloprotease, Tsp1-5, and Tsp1-8 domains of ADAMTS13. (A) Metalloprotease domain. The side chains of Arg193 and Arg268 are shown in blue with residue numbers. The active site zinc ion coordinated by His224, His228, and His234 is also shown (green). The mutations of H96D, R102C, T196I, L232Q, and S263C reported by Levy et al[12] and Schneppenheim et al[31] are present in the metalloprotease domain. The side chains of His96, Arg102, Thr196, Leu232, and Ser263 are also shown in blue. (B) Tsp1-5 domain. The side chains of Cys908 and Cys951 are shown in red with residue numbers. (C) Tsp1-8 domain. The side chain of Arg1123 is shown in red with residue number.

Discussion

Here, we have identified 7 new mutations in the *ADAMTS13* gene responsible for USS, including 4 missense mutations (R193W, I673F, C908Y, and R1123W) and 3 splice site mutations. We have reported 2 missense mutations (R268P and C508Y) and one nonsense mutation (Q449X).[18] All 6 missense mutant proteins, except for the R193W mutant, were not secreted from the cells in the expression analysis using HeLa cells. Although the R193W mutant was secreted to some extent, it had little activity. This mutation may not cause a dramatic conformational change of the enzyme but may disrupt the active site locally.

To date, the analysis of the *ADAMTS13* gene was reported in a total of 26 patients with congenital TTP, equivalent to USS, including those in the present study.[12,18,31-33] All of the patients with congenital TTP have been shown to have *ADAMTS13* gene mutations. Of these patients, 7 were homozygotes and 19 were compound heterozygotes. It is noteworthy that these mutation sites are distributed over exons 3 to 29 regardless of race. Among our 7 patients with USS, 2 are homozygotes, of whom 1 (patient C) has a family history of consanguineous marriage, and the other (patient B) appears not to have such a history. However, a careful routing analysis performed in this study revealed that 2 great-grandparents of patient B were from the same village in the Northeastern region of the Japanese mainland at the end of the 19th century. More interestingly, one Japanese patient with USS reported by Sasahara et al[34] has the same homozygous mutation (Q449X) as our patient B (personal written communication from Drs David Ginsburg and Shigeru Tsuchiya, May 2003). This patient is a natural habitant of the same Northeastern region of Japan as patient B's ancestors. Our experience suggests that among USS patients consanguinity gives rise to the minor group with homozygous mutation of the *ADAMTS13* gene, whereas the major group consists of individuals with compound heterozygous mutations not arising from consanguinity.

The most striking and earliest clinical sign of USS is a Coombs-test–negative severe hyperbilirubinemia soon after birth. In fact, all of our 7 patients had this history, and 6 of 7 were rescued by exchange blood transfusion and 1 by phototherapy. As noted by others[35] and by us,[16] some patients with USS, despite a severe lack of ADAMTS13 activity, have no acute episode of TTP/HUS during the newborn period, but develop the episode during early or late childhood. In some very unusual female cases, it has been said that the clinical manifestation is first noted after pregnancy.[35] This is perhaps triggered by an increased amount of VWF together with a higher ratio of ultralarge or large VWF multimers than in the nonpregnant state. However, it has not been clarified whether this phenomenon is caused by overproduction of VWF or by a physiologic decrease of ADAMTS13 activity during the second and third trimesters of normal pregnancy, and/or by both. At present we cannot address why phenotypic differences on the clinical onset or signs exist. Besides pregnancy, it has been

speculated that some other precipitating factors may include infections, cytokines, or chemical compounds.

In the present study, we constructed models of the metalloprotease domain, and Tsp1-5 and Tsp1-8 domains of ADAMTS13 using the coordinates of adamalysin II and the thrombospondin-1 type 1 repeats, respectively (Figure 5). The sequence alignments are highly important for obtaining the proper models. In the present study, the sequence alignments produced using PSI-BLAST were manually adjusted taking biologically important regions and secondary structure into consideration. Thus, the sequence identities of 22.1%, 28.8%, and 30.8% were obtained between the metalloprotease domain and adamalysin II, the Tsp1-5 domain and thrombospondin-1 type 1 repeats, and the Tsp1-8 domain and thrombospondin-1 type 1 repeats, respectively. Based on our experiences, the models constructed with the amino acid sequence identities higher than 20% are quite convincing. However, we did not construct the models of the cysteine-rich and spacer domains because their reference proteins were not obtained due to their unique sequences. In addition, the domain-domain interactions presumably present in the ADAMTS13 molecule are not predicted. Thus, the structure determined by the X-ray crystallography remains to be solved.

Acknowledgments

We thank Drs K. Kamide, S. Takiuchi, and Y. Kawano, Division of Hypertension and Nephrology, National Cardiovascular Center, for providing genomic DNAs isolated from individuals without TTP.

References

1. Moschcowitz E. Hyalin thrombosis of the terminal arterioles and capillaries: a hitherto undescribed disease. *Proc N Y Pathol Soc.* 1924;24:21-24.
2. Gasser C, Gautier E, Steck A, Siebenmann RE, Oechslin R. Hämolytisch-urämische Syndrome: bilaterale Nierenrindennekrosen bei akuten erworbenen hämolytischen Anämien. Schweiz Med Wochenschr. 1955;85:905-909.
3. Bell WR. Thrombotic thrombocytopenic purpura/hemolytic uremic syndrome relapse: frequency, pathogenesis, and meaning. Semin Hematol. 1997;34:134-139.
4. Furlan M, Robles R, Lämmle B. Partial purification and characterization of protease from human plasma cleaving von Willebrand factor to fragments produced by in vivo proteolysis. Blood. 1996;87:4223-4234.
5. Tsai HM. Physiologic cleavage of von Willebrand factor by a plasma protease is dependent on its conformation and requires calcium ion. Blood. 1996;87:4235-4244.
6. Furlan M, Robles R, Galbusera M, et al. von Willebrand factor-cleaving protease in thrombotic thrombocytopenic purpura and the hemolytic-uremic syndrome. N Engl J Med. 1998;339:1578-1584.
7. Tsai HM, Lian ECY. Antibodies to von Willebrand factor-cleaving protease in acute thrombotic thrombocytopenic purpura. N Engl J Med. 1998; 339:1585-1594.
8. Gerritsen H, Robles R, Lämmle B, Furlan M. Partial amino acid sequence of purified von Willebrand factor-cleaving protease. Blood. 2001;98: 1654-1661.
9. Fujikawa K, Suzuki H, McMullen B, Chung D. Purification of human vWF-cleaving protease and its identification as a new member of the metalloproteinase family. Blood. 2001;98:1662-1666.
10. Zheng X, Chung D, Takayama TK, Majerus EM, Sadler JE, Fujikawa K. Structure of von Willebrand factor cleaving protease (ADAMTS13), a metalloprotease involved in thrombotic thrombocytopenic purpura. J Biol Chem. 2001;276: 41059-41063.
11. Soejima K, Mimura N, Hirashima M, et al. A novel human metalloprotease synthesized in the liver and secreted into the blood: possibly, the von Willebrand factor-cleaving protease? J Biochem. 2001;130:475-480.
12. Levy GG, Nichols WC, Lian E, et al. Mutations in a member of the ADAMTS gene family cause thrombotic thrombocytopenic purpura. Nature. 2001;413:488-494.
13. Schulman I, Pierce M, Likens A, Currimbhoy Z. Studies on thrombopoiesis: I. a factor in normal human plasma required for platelet production; chronic thrombocytopenia due to its deficiency. Blood. 1960;14:943-957.
14. Upshaw JD. Congenital deficiency of a factor in normal plasma that reverses microangiopathic hemolysis and thrombocytopenia. N Engl J Med. 1978;298:1350-1352.
15. Kinoshita S, Yoshioka A, Park YD, et al. Upshaw-Schulman syndrome revisited: a concept of congenital thrombotic thrombocytopenic purpura. Int J Hematol. 2001;74:101-108.
16. Fujimura Y, Matsumoto M, Yagi H, Yoshioka A, Matsui T, Titani K. von Willebrand factor-cleaving protease and Upshaw-Schulman syndrome. In: Progress in Hematology. Int J Hematol. 2002;75: 25-34.
17. Furlan M, Robles R, Solenthaler M, Wassmer M, Sandoz P, Lämmle B. Deficient activity of von Willebrand factor-cleaving protease in chronic relapsing thrombotic thrombocytopenic purpura. Blood. 1997;89:3097-3103.
18. Kokame K, Matsumoto M, Soejima K, et al. Mutations and common polymorphisms in *ADAMTS13* gene responsible for von Willebrand factor-cleaving protease activity. Proc Natl Acad Sci U S A. 2002;99:11902-11907.
19. Miura M, Koizumi S, Nakamura K, et al. Efficiency of several plasma components in a young boy with chronic thrombocytopenia and hemolytic anemia who responds repeatedly to normal plasma infusions. Am J Hematol. 1984;17:307-319.
20. Shinohara T, Miyamura S, Suzuki E, Kobayashi K. Congenital microangiopathic hemolytic anemia: report of Japanese girl. Eur J Pediatr. 1982; 138:191-193.
21. Mori Y, Wada H, Gabazza EC, et al. Predicting response to plasma exchange in patients with thrombotic thrombocytopenic purpura with measurement of vWF-cleaving protease activity. Transfusion. 2002;42:572-580.
22. Niwa H, Yamamura K, Miyazaki J. Efficient selection for high-expression transfectants with a novel eukaryotic vector. Gene. 1991;108:193-199.
23. Altschul SF, Madden TL, Schaffer AA, et al. Gapped BLAST and PSI-BLAST: a new generation of protein database search programs. Nucleic Acids Res. 1997;25:3389-3402.
24. Berman HM, Westbrook J, Feng Z, et al. The Protein Data Bank. Nucleic Acids Res. 2000;28:235-242.
25. Cirilli M, Gallina C, Gavuzzo E, et al. 2 angstrom X-ray structure of adamalysin II complexed with a peptide phosphonate inhibitor adopting a retro-binding mode. FEBS Lett. 1997;418:319-322.
26. Tan K, Duquette M, Liu JH, et al. Crystal structure of the TSP-1 type 1 repeats: a novel layered fold and its biological implication. J Cell Biol. 2002; 159:373-382.
27. Yoneda T, Komooka H, Umeyama H. A computer modeling study of the interaction between tissue factor pathway inhibitor and blood coagulation factor Xa. J Protein Chem. 1997;16:597-605.
28. Takeda-Shitaka M, Umeyama H. Elucidation of the cause for reduced activity of abnormal human plasmin containing an Ala55-Thr mutation: importance of highly conserved Ala55 in serine proteases. *FEBS Lett.* 1998;425:448-452.
29. Ogata K, Umeyama H. An automatic homology modeling method consisting of database searches and simulated annealing. J Mol Graph Model. 2000;18:258-272.
30. Iwadate M, Ebisawa K, Umeyama H. Comparative modeling of CAFASP2 competition. Chem-Bio Info J. 2001;1:136-148.
31. Schneppenheim R, Budde U, Oyen F, et al. von Willebrand factor cleaving protease and ADAMTS13 mutations in childhood TTP. Blood. 2003;101:1845-1850.
32. Savasan S, Lee SK, Ginsburg D, Tsai HM. *ADAMTS13* gene mutations in congenital thrombotic thrombocytopenic purpura with previously reported normal VWF cleaving protease activity. Blood. 2003;101:4449-4451.
33. Antoine G, Zimmermann K, Plaimauer B, et al. *ADAMTS13* gene defects in two brothers with constitutional thrombotic thrombocytopenic purpura and normalization of von Willebrand factor-cleaving protease activity by recombinant human ADAMTS13. Br J Haematol. 2003;120:821-824.
34. Sasahara Y, Kumaki S, Ohashi Y, et al. Deficient activity of von Willebrand factor-cleaving protease in patients with Upshaw-Schulman syndrome. Int J Hematol. 2001;74:109-114.
35. Furlan M, Lämmle B. Aetiology and pathogenesis of thrombotic thrombocytopenic purpura and haemolytic uraemic syndrome: the role of von Willebrand factor-cleaving protease. Best Pract Res Clin Haematol. 2001;14:437-454.

MOLECULAR AND CELLULAR BIOLOGY, May 2004, p. 3949–3956 Vol. 24, No. 9
0270-7306/04/$08.00+0 DOI: 10.1128/MCB.24.9.3949–3956.2004

Ndrg1-Deficient Mice Exhibit a Progressive Demyelinating Disorder of Peripheral Nerves

Tomohiko Okuda,[1] Yujiro Higashi,[2] Koichi Kokame,[1] Chihiro Tanaka,[1] Hisato Kondoh,[2] and Toshiyuki Miyata[1]*

National Cardiovascular Center Research Institute, Suita, Osaka 565-8565,[1] and Laboratory of Developmental Biology, Graduate School of Frontier Bioscience, Osaka University, Suita, Osaka 565-0871,[2] Japan

Received 28 August 2003/Returned for modification 3 November 2003/Accepted 10 January 2004

NDRG1 is an intracellular protein that is induced under a number of stress and pathological conditions, and it is thought to be associated with cell growth and differentiation. Recently, human *NDRG1* was identified as a gene responsible for hereditary motor and sensory neuropathy-Lom (classified as Charcot-Marie-Tooth disease type 4D), which is characterized by early-onset peripheral neuropathy, leading to severe disability in adulthood. In this study, we generated mice lacking *Ndrg1* to analyze its function and elucidate the pathogenesis of Charcot-Marie-Tooth disease type 4D. Histological analysis showed that the sciatic nerve of *Ndrg1*-deficient mice degenerated with demyelination at about 5 weeks of age. However, myelination of Schwann cells in the sciatic nerve was normal for 2 weeks after birth. *Ndrg1*-deficient mice showed muscle weakness, especially in the hind limbs, but complicated motor skills were retained. In wild-type mice, NDRG1 was abundantly expressed in the cytoplasm of Schwann cells rather than the myelin sheath. These results indicate that NDRG1 deficiency leads to Schwann cell dysfunction, suggesting that NDRG1 is essential for maintenance of the myelin sheaths in peripheral nerves. These mice will be used for future analyses of the mechanisms of myelin maintenance.

NDRG1, an intracellular protein composed of 394 amino acids, is highly conserved among multicellular organisms, and its expression is induced by stress stimuli. Previously, we showed that NDRG1 is induced by homocysteine, 2-mercaptoethanol, and tunicamycin in cultured human endothelial cells (13). This pattern is similar to that seen for molecular chaperones in the endoplasmic reticulum. Subsequently, NDRG1 was found to be upregulated in a human lung cells following treatment with nickel compounds (31). This change in expression reflected an increase in hypoxia-inducible factor 1 caused by hypoxia or the subsequent elevation of intercellular calcium concentrations (23, 24). NDRG1 expression is also induced by p53 expression and DNA damage, and its expression is inhibited under conditions of cell growth (14). These results suggest that NDRG1 is involved in the cellular stress response mechanisms.

Conversely, *Ndrg1* was also identified as a downstream target of N-*myc* (25). In N-*myc* knockout mouse embryos, NDRG1 expression is upregulated. During the early stages of differentiation of some tissues, it seems that N-myc activity leads to decreased NDRG1 expression as tissue differentiation progresses. Indeed, *NDRG1* has been identified as a gene whose expression is downregulated in tumors (14, 27). Furthermore, NDRG1 expression is induced by differentiation stimuli in cancer cells (21, 29). *NDRG1* was also reported to be a metastasis suppressor gene (3, 6). In this regard, the effects of *NDRG1* are thought to reflect its potential role in cell differentiation.

Recently, a nonsense mutation of human *NDRG1* was reported to be causative for hereditary motor and sensory neuropathy-Lom (9), which is a severe peripheral neuropathy identified in the Gypsy community of Lom, a small town in northwest Bulgaria (10, 11). The hereditary motor and sensory neuropathy-Lom is classified as Charcot-Marie-Tooth disease type 4D (4). Patients with this disease exhibit an early-onset peripheral neuropathy that progresses to severe disability in adulthood, characterized by muscle weakness, sensory loss, and neural deafness. These symptoms are caused by demyelination of peripheral nerves. These observations suggest that NDRG1 is necessary for axonal survival.

To clarify the function(s) of NDRG1, we generated *Ndrg1*-deficient mice by gene targeting. The *Ndrg1*-deficient mice exhibited progressive demyelination in peripheral nerves. Moreover, we showed that NDRG1 was significantly expressed in the cytoplasm of Schwann cells, suggesting that NDRG1 deficiency is a primary cause of Schwann cell dysfunction.

MATERIALS AND METHODS

Construction of targeting vector. We isolated genomic clones carrying the mouse *Ndrg1* gene and characterized the promoter and the first exon (25). An 8.9-kb EcoRI fragment encompassing the promoter and exon 1 was used to construct the targeting vector. The initiating Met codon for NDRG1 translation exists in exon 2. A *loxP*-flanked pSTneoB (26) cassette was inserted at the BamHI site 1.2 kb downstream of the transcriptional start site, and an additional *loxP* plus BamHI site sequence was inserted at an EcoRV site 1.2 kb upstream of the start site. This resulted in three *loxP* sites in the vector, so that the Cre recombinase should excise the promoter and exon 1 (Fig. 1A). The sequence was inserted into the diphtheria toxin A fragment cassette vector (30), and the DNA was linearized by SalI digestion for electroporation.

* Corresponding author. Mailing address: National Cardiovascular Center Research Institute, 5-7-1 Fujishirodai, Suita, Osaka 565-8565, Japan. Phone: 81-6-6833-5012, ext. 2512. Fax: 81-6-6835-1176. E-mail: miyata@ri.ncvc.go.jp.

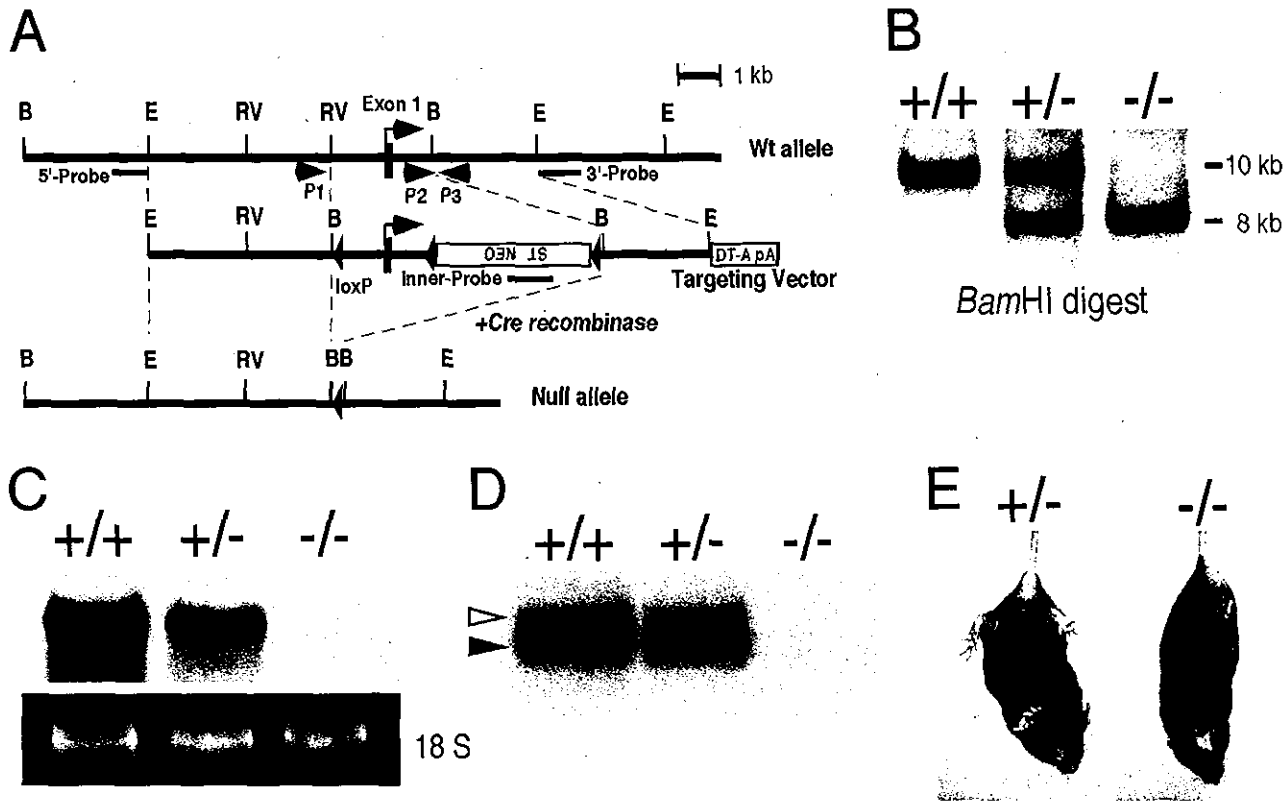

FIG. 1. Targeted disruption of *Ndrg1*. (A) Targeting strategy for the *Ndrg1* gene. Solid boxes represent exon 1 of *Ndrg1*. Arrowheads indicate the location and orientation of *loxP* sites. The *loxP*-flanked pSTneoB cassette (ST NEO) and the third *loxP* sequence were inserted into the targeting vector. A diphtheria toxin A fragment cassette with a polyadenylation signal (DT-A pA) was included at the 3′ end of the vector for negative selection of ES cells. 5′-External, 3′-external, and inner probes for selection of ES clones by Southern blotting are shown as bars. PCR primers to discriminate each allele are shown as P1, P2, and P3. B, BamHI; E, EcoRI; RV, EcoRV. (B) Southern blot analysis. Genomic DNA was prepared from littermates obtained by heterozygous intercrossing and subjected to BamHI digestion. The wild-type and null alleles gave about 10- and 8-kb bands, respectively, with the 5′ probe. (C) Northern blot analysis of the kidneys from 2-month-old male mice. The partial mouse *Ndrg1* cDNA fragment (904 bp) was used as a specific probe. Equal loading among lanes was confirmed by staining of 18 S rRNA. *Ndrg1* mRNA expression was not detected in $Ndrg1^{-/-}$ mice. (D) Western blot analysis of the kidneys from 2-month-old male mice. Each lane contains 5 μg of total protein. NDRG1 expression was partially reduced in the $Ndrg1^{+/-}$ mouse and absent in the $Ndrg1^{-/-}$ mouse. The majority of NDRG1 was detected at an apparent molecular mass of 43 kDa (solid arrowhead). The upper bands indicate phosphorylated NDRG1 (open arrowhead). (E) A phenotype in the appearance of an $Ndrg1^{-/-}$ mouse at 3 months of age. An abnormal hind limb clasping phenotype was seen in $Ndrg1^{-/-}$ mice upon tail suspension, indicating neurological abnormalities.

Generation of *Ndrg1*-null mutant mice. R1 embryonic stem (ES) cells (18) were electroporated with the targeting vector and selected with 250 μg of G418 per ml. G418-resistant ES colonies were selected, and correctly targeted clones were identified by Southern blotting with a Gene Images Random-Prime system (Amersham Biosciences) with 5′-external, 3′-external, and inner probes (Fig. 1A). These ES cells were injected into blastocysts to obtain mouse chimeras, which were crossed with wild-type C57BL/6 mice (SLC Japan) for germ line transmission of the floxed *Ndrg1* allele. These mice were further crossed with *EIIa-Cre* deleter mice (15) to excise the promoter and exon 1 region of the *Ndrg1* gene together with the neomycin resistance cassette (7). Successful excision of the sequences in the offspring was confirmed by PCR analysis of DNA isolated from punctured ear lobes with primers P1 (5′-AGCAGGCTCTTAAAGCGGC TCC-3′), P2 (5′-CCGCCTCTGTCAAATTAGTAGCTG-3′), and P3 (5′-GGG AGAGCTGAAGGCTGTTCTAGG-3′). Those heterozygous mice with the excised *Ndrg1* allele were backcrossed with wild-type C57BL/6 mice. The heterozygous offspring lacking the *Cre* gene were used for this study. The experiments were conducted in accordance with the current guidelines for the care and use of experimental animals of the National Cardiovascular Center in Japan.

Northern blot analysis. Male mice aged 2 months (wild-type, heterozygous, and homozygous mice) were sacrificed, and their kidneys and sciatic nerves were excised. For extraction of total RNA, whole kidneys or sciatic nerves were immediately homogenized in Trizol reagent (Invitrogen). Isolated total RNA was electrophoresed in a 1% agarose gel containing 2% formaldehyde (10 μg/lane) and transferred to a nylon membrane. To make a specific probe, a partial cDNA fragment (904 bp) was amplified by PCR with primers 5′-CTCAGACA CCAAACTGCCAAAAC-3′ and 5′-AATGCTACAAACCCAGTCAGCAG-3′, with the full-length *Ndrg1* cDNA used as a template. The fragment obtained was labeled with fluorescein-12-dUTP (PerkinElmer Life Sciences), and hybridization and detection procedures were performed as previously described (32).

Western blot analysis. For extraction of total protein, the excised organs were homogenized in lysis buffer as described before (12). The protein lysates were subjected to sodium dodecyl sulfate-polyacrylamide gel electrophoresis (10 to 20% gradient gel) and transferred to a polyvinylidene difluoride membrane (Bio-Rad). After blocking with 3% skim milk in phosphate-buffered saline (PBS) with 0.05% Tween 20, the membrane was incubated with a 1:1,000 dilution of anti-NDRG1 antiserum (2) and then with a 1:1,000 dilution of peroxidase-conjugated goat anti-rabbit immunoglobulin G (Zymed). Detection was performed with the Western Lightning Chemiluminescence Reagent Plus (PerkinElmer Life Sciences) with the LAS-1000plus image analyzer.

Histological analyses. Male mice aged 1, 2, and 5 weeks and 3 and 6 months (wild-type, heterozygous, and homozygous mice) were anesthetized with nembutal (Abbott Laboratories) and perfused with ice-cold PBS containing 4% paraformaldehyde, and sciatic nerve fragments were excised. For light and electron microscopy, the fragments were fixed with 2.5% glutaraldehyde for 2 h at 4°C. After being washed with PBS, the samples were cut into small pieces and fixed with 2% OsO_4 for 2 h at 4°C. After dehydration in an ascending ethanol series, the samples were embedded in Quetol812 resin. For light microscopy, semithin sections (1-μm thickness) of sciatic nerves were stained with 0.1%

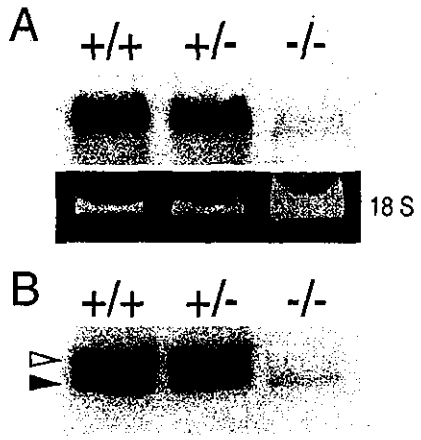

FIG. 2. Leaky expression of NDRG1 in the sciatic nerve of *Ndrg1*$^{-/-}$ mice. (A) Northern blot analysis of the sciatic nerves from mice at 2 months of age. 18 S rRNA was used as an internal control. (B) Western blot analysis of the sciatic nerves from mice at 2 months of age. Each lane contains 5 μg of total protein. NDRG1 was detected at 43 kDa (solid arrowhead). The upper bands indicate phosphorylated NDRG1 (open arrowhead). Low-level expression of NDRG1 was detected in the sciatic nerves of *Ndrg1*$^{-/-}$ mice.

toluidine blue. Slides were examined with an Axioplan 2 microscope (Carl Zeiss). For electron microscopy, ultrathin sections (90-nm thickness) on mesh grids were stained with uranyl acetate and lead acetate and examined with an H-300 electron microscope (Hitachi).

For immunofluorescence microscopy, paraformaldehyde-fixed sciatic nerve specimens from mice aged 3 weeks (wild-type and homozygous mice) were washed with PBS at 4°C and embedded in OCT compound (Sakura Finetek) at −80°C. Frozen sections (5-μm thickness) were washed with PBS. After being blocked with 10% normal goat serum for 15 min at room temperature, the sections were incubated with a 1:200 dilution of anti-NDRG1 antiserum and a 1:100 dilution of rat anti-myelin basic protein (MBP) monoclonal antibody (Chemicon) overnight at 4°C and then with a 1:100 dilution of Alexa Fluor 488-conjugated anti-rabbit immunoglobulin G antibody (Molecular Probes) and a 1:100 dilution of Alexa Fluor 546-conjugated anti-rat immunoglobulin G antibody (Molecular Probes) for 1 h at room temperature. Fluorescence was detected with the Axiovert 200 microscope and photographed with the AxioCam (Carl Zeiss).

Quantitative analysis of demyelination. Semithin sections of sciatic nerves from three homozygous and three wild-type mice aged 3 weeks and 3 months were photographed, and myelinated axons in a fixed area were counted manually. The diameter of the axons and the thickness of nerve fibers (axon plus myelin) were analyzed with ImageGauge software (Fujifilm). To assess the thickness of the myelin sheath, the g ratio (axon diameter/fiber diameter) was calculated (1, 5). Complex figures with folded myelin were excluded. The significance of differences between mean values was determined by the *F* test.

RT-PCR analysis. Total RNA was extracted from the sciatic nerves, kidneys, and brains of homozygous and wild-type mice aged 5 weeks. Reverse transcription-PCR (RT-PCR) was performed with total RNA (50 ng) as the template and a SuperScript One-Step RT-PCR kit with Platinum *Taq* (Invitrogen). The primer pairs were 5′-ACCCTGAGATGGTAGAGGGTCTC-3′ and 5′-CCAATTTAG AATTGCATTCCACC-3′ for *Ndrg1*, 5′-ATTCTTGGACATCTTTTCAGCC A-3′ and 5′-TGCAGGAAGTACTTGAAAGCCTC-3′ for *Ndrg2*, 5′-CATTAA CATTGACCCGTGTGCTA-3′ and 5′-TTGTATTTATAGGGTCGAGGCG A-3′ for *Ndrg3*, 5′-AAGTACGTGATTGGCATTGGAGT-3′ and 5′-CAGGTG CATTATCTCCGACTACC-3′ for *Ndrg4*, and 5′-GGAGAAACCTGCCAAGT ATGATG-3′ and 5′-CTAGGCCCCTCCTGTTATTATGG-3′ for *Gapd*.

Motor activity tests. In the wire-hanging test, we assessed the grip strength of the mice as described before (8). Each mouse was placed on wire netting (20 by 30 cm) taped around the edge. The wire netting was shaken three times and turned upside down. The amount of time that each mouse held onto the wire netting was recorded up to a maximum of 300 s. In the rotorod test, we assessed the ability of the mice to maintain balance on a rotating cylinder as described before (17). The accelerating Rota-Rod (model 7650; Ugo Basile) consists of a 3-cm-diameter cylinder with knurls. Each mouse was placed on the cylinder, which turned at a constant rotation (5 rpm) for 1 min for training, and then the

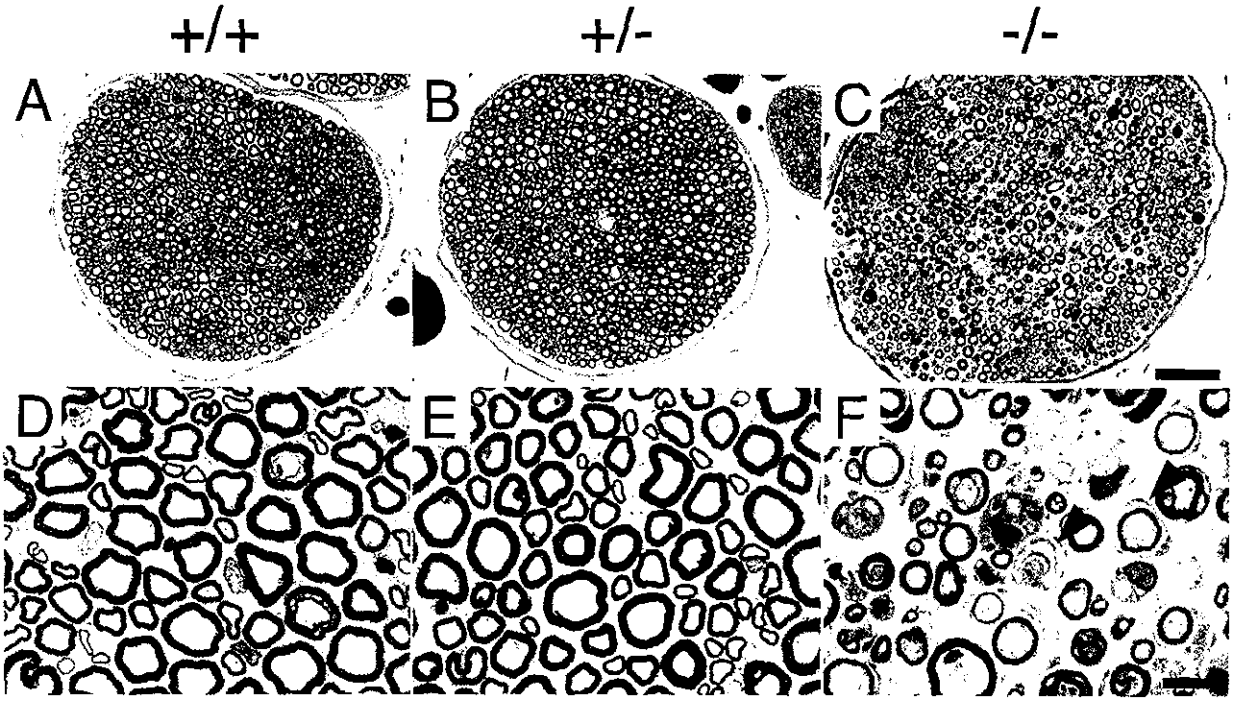

FIG. 3. Histological examination of sciatic nerves. Transverse sections of the sciatic nerves from *Ndrg1*$^{+/+}$ (A and D), *Ndrg1*$^{+/-}$ (B and E), and *Ndrg1*$^{-/-}$ (C and F) mice at 3 months of age are shown. Panels D, E, and F are higher magnifications of panels A, B, and C, respectively. The sciatic nerves of the *Ndrg1*$^{-/-}$ mouse (C and F) showed features typical of demyelinating neuropathy. Many thinly myelinated axons and onion bulb degeneration were seen (arrowheads). No difference was observed between *Ndrg1*$^{+/+}$ and *Ndrg1*$^{+/-}$ mice. Bars, 50 μm (A to C); 10 μm (D to F).

TABLE 1. Quantitative analysis of sciatic nerve[a]

Age	*Ndrg1* genotype	Mean axon density (10^4/mm^2) ± SD	Mean axon diam (μm) ± SD	Mean g ratio ± SD (no. of fibers)
3 wk	+/+	2.65 ± 0.23	3.46 ± 0.97	0.67 ± 0.06 (980)
	−/−	2.87 ± 0.22	3.09 ± 0.82*	0.66 ± 0.06 (1,028)
3 mo	+/+	2.45 ± 0.32	4.13 ± 1.41	0.67 ± 0.06 (760)
	−/−	1.61 ± 0.12*	3.19 ± 1.09*	0.73 ± 0.09* (661)

[a] *, statistically different from $Ndrg1^{+/+}$ mice of the same age ($P < 0.05$).

rotation speed was increased over a 300-s period from 5 to 30 rpm. The amount of time that the mouse remained on the accelerating cylinder was recorded. Mice that fell in less than 15 s were given a second trial. Mice that did not fall during the 300-s trial period were given a score of 300 s. Two sets of the rotorod test were performed in the same day, and the higher score for each mouse is reported. The body weight of each mouse was also measured. Both motor activity tests were carried out once every 2 weeks from 5 to 19 weeks of age.

RESULTS

Generation of *Ndrg1*-deficient mice. We made a targeting vector to eliminate *Ndrg1* expression by deletion of the promoter and exon 1 region with *Cre-loxP* excision (Fig. 1A). R1 ES cells were electroporated with the targeting vector and selected with G418. One hundred forty-five G418-resistant ES colonies were selected, and correctly targeted clones were identified by Southern blotting with a 5′-external sequence probe (Fig. 1A and B). Five independently targeted clones were isolated, and the genomic organization of their *Ndrg1* locus was further confirmed by Southern blotting with 3′-external and internal probes. After *Cre-loxP* excision, two lines of mice heterozygous for deletion of the *Ndrg1* promoter and exon 1 were obtained. Mice with the deleted *Ndrg1* allele and without the *Cre* gene ($Ndrg1^{+/-}$) were backcrossed with wild-type C57BL/6 mice ($Ndrg1^{+/+}$). The $Ndrg1^{+/-}$ mice were crossed to generate homozygous *Ndrg1*-deficient mice ($Ndrg1^{-/-}$).

Phenotype of *Ndrg1*-deficient mice. $Ndrg1^{-/-}$ mice were born normally with the expected Mendelian frequency. Both male and female $Ndrg1^{-/-}$ mice were fertile. We confirmed the elimination of NDRG1 expression in the kidney, where NDRG1 was abundantly expressed in wild-type mice (Fig. 1C and D) (32). However, in the sciatic nerve, a faint signal of *Ndrg1* mRNA was detectable in $Ndrg1^{-/-}$ mice by Northern blot analysis (Fig. 2A). Leaky transcription of NDRG1 might be possible because the $Ndrg1^{-/-}$ mice still showed normal organization of the *Ndrg1* gene downstream of exon 2, containing the initiating Met codon. To confirm this possibility, we performed Western blot analysis on lysates from the sciatic nerves of $Ndrg1^{+/+}$, $Ndrg1^{+/-}$, and $Ndrg1^{-/-}$ mice. As shown in Fig. 2B, faint bands corresponding to the normal size of NDRG1 were observed. These data suggested that a small amount of full-length NDRG1 was expressed in the sciatic nerves of $Ndrg1^{-/-}$ mice. In this regard, $Ndrg1^{-/-}$ mice are hypomorphic, at least in the sciatic nerves.

Despite the low-level expression of NDRG1, $Ndrg1^{-/-}$ mice began showing hind limb weakness at 3 months of age. We also detected an abnormal limb clasping phenotype in $Ndrg1^{-/-}$ mice upon tail suspension (Fig. 1E). These observations suggested neurological abnormalities. These phenotypes were progressive, that is, 1-year-old or older $Ndrg1^{-/-}$ mice exhibited substantial impairment in hind limb function (i.e., dragging of their legs) and leg muscle atrophy. Two independent lines of $Ndrg1^{-/-}$ mice exhibited similar phenotypes. $Ndrg1^{+/-}$ mice were indistinguishable from $Ndrg1^{+/+}$ mice in both appearance and behavior.

Peripheral nerve degeneration of *Ndrg1*-deficient mice. To address possible peripheral nerve dysfunction, we performed histological analyses. Severe degeneration of the sciatic nerves in $Ndrg1^{-/-}$ mice was seen at 3 months of age. We observed a large number of thinly myelinated axons (Fig. 3C and F). The myelinated axons were significantly decreased in density, and the g ratios of the neuronal fibers were significantly increased in $Ndrg1^{-/-}$ mice at 3 months of age (Table 1). Electron microscopy of the sciatic nerve showed onion bulb pathology with Schwann cell processes, thin myelin sheaths, endoneurial collagenization, and infiltration of macrophages in $Ndrg1^{-/-}$ mice (Fig. 4C). A similar demyelinating phenotype is seen in human Charcot-Marie-Tooth disease type 4D patients (11).

To investigate the process of demyelination in $Ndrg1^{-/-}$ mice, we assessed the initial formation of the neuronal myelin sheath at a younger age. Histological analysis showed that, at 1 and 2 weeks of age, the sciatic nerves of $Ndrg1^{-/-}$ mice did not differ from the nerves of $Ndrg1^{+/+}$ mice; both displayed normal

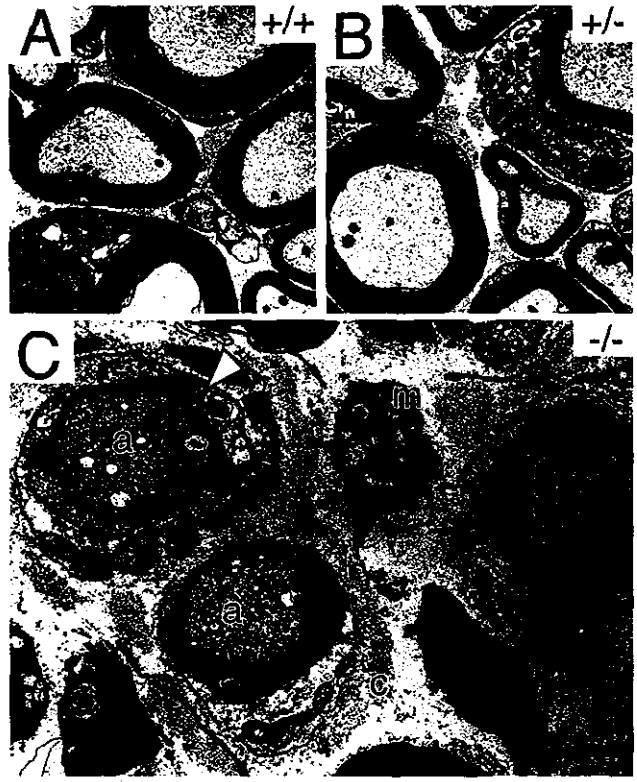

FIG. 4. Electron microscopy of sciatic nerves. Electron micrographs of the sciatic nerves from $Ndrg1^{+/+}$ (A), $Ndrg1^{+/-}$ (B), and $Ndrg1^{-/-}$ (C) mice at 3 months of age were shown. Onion bulb pathology with Schwann cell processes (*open arrowhead*), axons with thin myelin sheath (a), excess collagenization (c), and infiltration of macrophages (m) were observed in $Ndrg1^{-/-}$ mice. Bar, 2 μm.

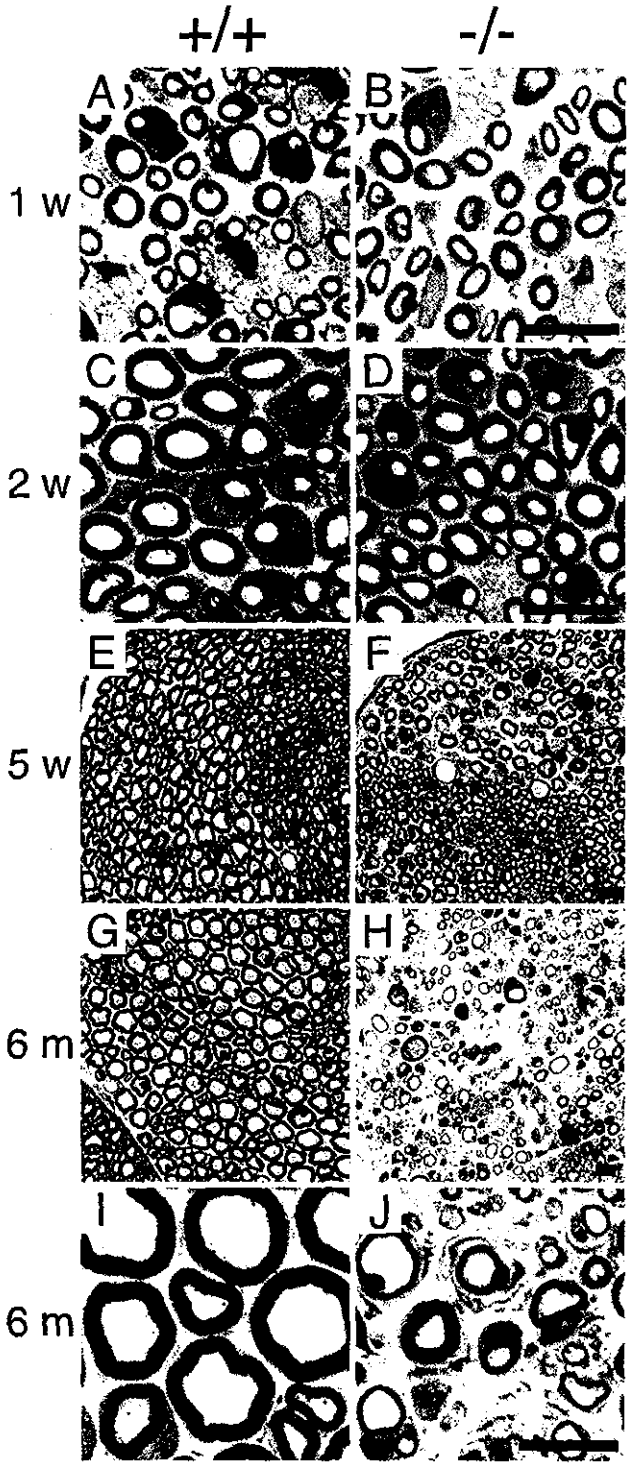

FIG. 5. Time course analysis of sciatic nerves during growth. Transverse sections of the sciatic nerves from *Ndrg1*$^{+/+}$ (A, C, E, G, and I) and *Ndrg1*$^{-/-}$ (B, D, F, H, and J) mice were compared. These specimens were derived from mice of the following ages: A and B, 1 week; C and D, 2 weeks; E and F, 5 weeks; and G to J, 6 months. Panels I and J are higher magnifications of panels G and H, respectively. At 1 to 2 weeks of age, Schwann cell proliferation and myelin formation were normal, and no demyelination was observed in *Ndrg1*$^{-/-}$ mice. However, at 5 weeks of age, partial degeneration of the sciatic nerves had occurred in *Ndrg1*$^{-/-}$ mice, especially in relatively thick axons. At 6 months of age, degeneration of the sciatic nerves had progressed further, with an apparent reduction of myelinated axons in *Ndrg1*$^{-/-}$ mice. Bars, 10 μm.

growth of Schwann cells and normal formation of the myelin sheath (Fig. 5A to D). At 3 weeks of age, the density of myelinated axons was not affected in *Ndrg1*$^{-/-}$ mice, and no significant difference in the g ratios was observed (Table 1). However, at 5 weeks of age, the myelin sheaths of *Ndrg1*-deficient mice began to degenerate (Fig. 5F). The observed demyelination was incomplete and sporadic but was especially pronounced in the myelin sheaths of relatively thick axons. These results indicated that Schwann cell proliferation and myelination were normal and that some defect in the maintenance of the myelin sheath occurred in *Ndrg1*$^{-/-}$ mice. Older *Ndrg1*$^{-/-}$ mice exhibited more severe disease in their sciatic nerves, demonstrating that this peripheral nerve degeneration is progressive (Fig. 5G to J).

NDRG1 is ubiquitously expressed in various tissues (13, 32). In particular, the kidney is reported to be a site of high NDRG1 expression in mice and humans (16, 32). Although the peripheral nerves of *Ndrg1*$^{-/-}$ mice demonstrated clear pathology, no apparent morphological abnormality was observed in their kidneys (data not shown).

Localization of NDRG1 protein in the sciatic nerve. To examine which cells, neurons or Schwann cells, are responsible for the demyelinating defects, we investigated the expression of NDRG1 in the sciatic nerve by immunohistochemical analysis. At 3 weeks of age, NDRG1 was abundantly expressed in the cytoplasm of Schwann cells rather than in myelin sheaths or axons in *Ndrg1*$^{+/+}$ mice (Fig. 6A to C). We confirmed that MBP, a myelin marker protein, was normally expressed in the myelin sheath of the sciatic nerves of both *Ndrg1*$^{+/+}$ and *Ndrg1*$^{-/-}$ mice (Fig. 6B and E). These results suggested that the cytoplasmic expression of NDRG1 in Schwann cells is essential for the maintenance of myelin structure. Thus, defects in Schwann cells caused by NDRG1 deficiency could be a primary cause of the neural degeneration seen in *Ndrg1*$^{-/-}$ mice.

Expression of other NDRG family members. To compare the expression patterns of all NDRG family members, we performed RT-PCR analysis on RNA samples from the sciatic nerve, brain, and kidney of *Ndrg1*$^{+/+}$ and *Ndrg1*$^{-/-}$ mice (Fig. 7). In *Ndrg1*$^{+/+}$ mice, *Ndrg1* was expressed in the sciatic nerves as much as in the kidney but relatively less expressed in the brain. In contrast, *Ndrg2*, *Ndrg3*, and *Ndrg4* were abundantly expressed in the brain of both *Ndrg1*$^{+/+}$ and *Ndrg1*$^{-/-}$ mice but less in the sciatic nerves. Upregulation of *Ndrg2*, *Ndrg3*, and *Ndrg4* was not observed in *Ndrg1*$^{-/-}$ mice.

Muscle strength and motor activity of *Ndrg1*-deficient mice. To examine the muscle strength of the legs, the wire-hanging test was performed. *Ndrg1*$^{-/-}$ mice were able to hang onto the wire for a significantly shorter period than *Ndrg1*$^{+/+}$ at all ages tested. *Ndrg1*$^{-/-}$ mice demonstrated that their muscle strength was quite decreased. Male mice of both genotypes tended to fall sooner than females due to their heavier body weight (Fig. 8A and C). To measure more complicated motor activities and motor learning in the same mice, a rotorod test was carried out. The scores of older *Ndrg1*$^{-/-}$ mice in this test were slightly lower than those of the age-matched *Ndrg1*$^{+/+}$ controls, though the differences were minor compared to those seen in the wire-hanging test (Fig. 8B).